Celígo® S *Applications Collection*

Adherent Cell Cytometer

Minimally Invasive, Microplate-Based Cytometry

1. IMAGE ····► 2. ANALYZE ····► 3. RESULTS

whole well — cell images — data curves & cell images

384-well
96-well
48-well
24-well
6-well
T Flask

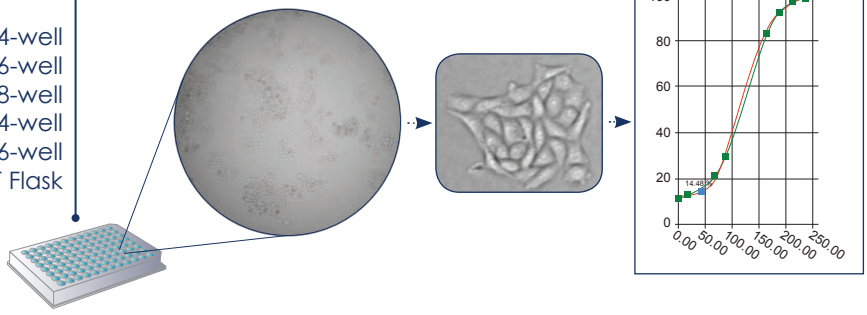

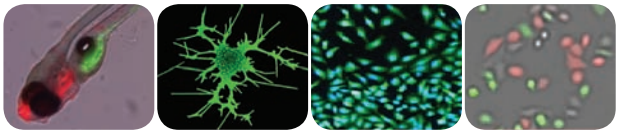

Nexcelom Bioscience

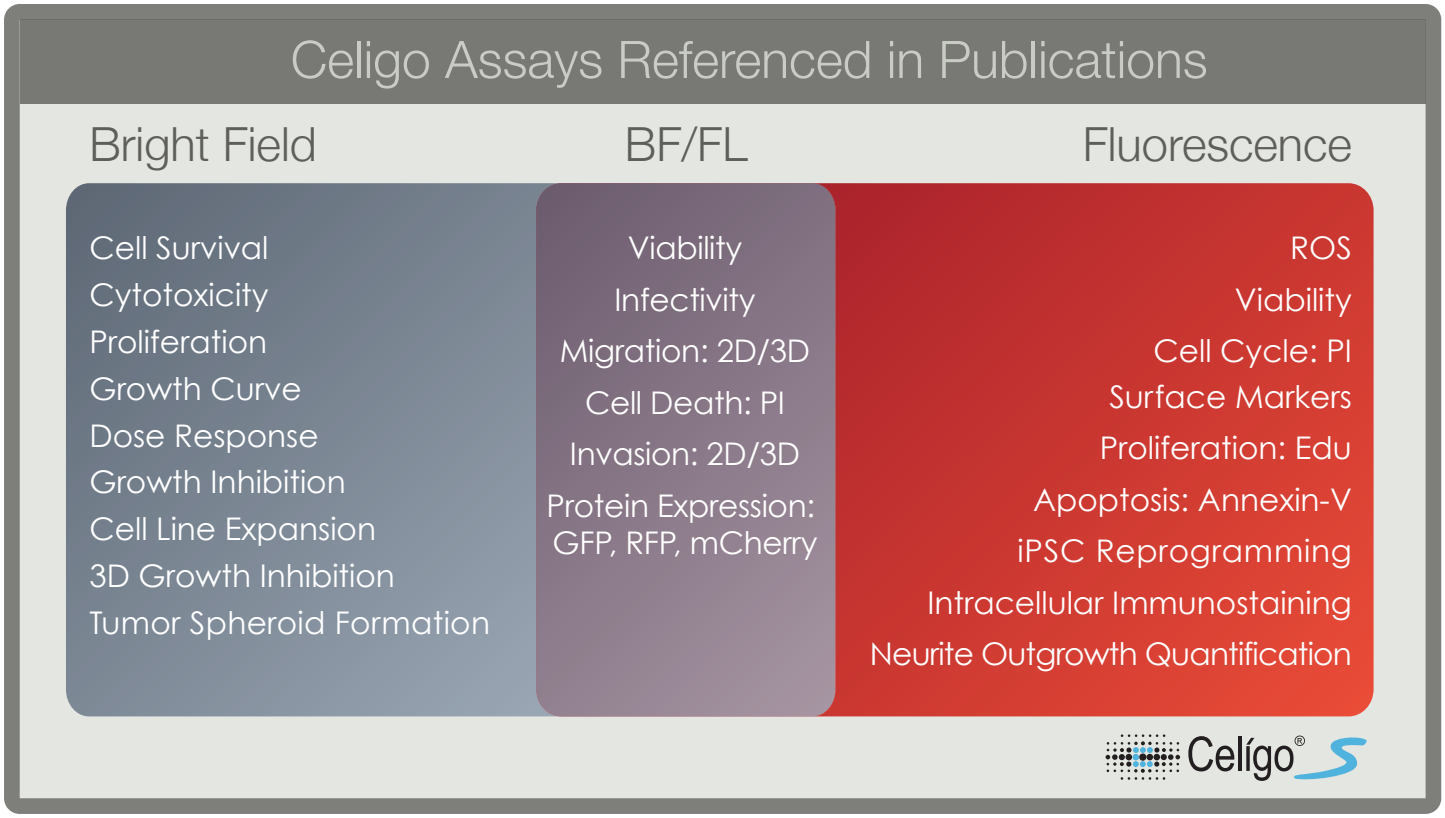

Table of Contents

Automated Cell Growth Tracking for Cytotoxicity, Proliferation

Celigo® S

Label-Free, Non-Destructive, No Need to Trypsinize Adherent Cells

The Growth Tracking application automatically integrates label-free cell counts of the same well/flask from different time points to provide direct measurement of growth rates and doubling times, which is also a good overall assessment of cell health.

Two Methods to Produce a Label-Free Proliferation Curve

Method 1

The first method is to use cell segmentation, where each cell is identified by the image analysis software to produce a cell count. This method requires customization of the analysis parameters for each cell type.

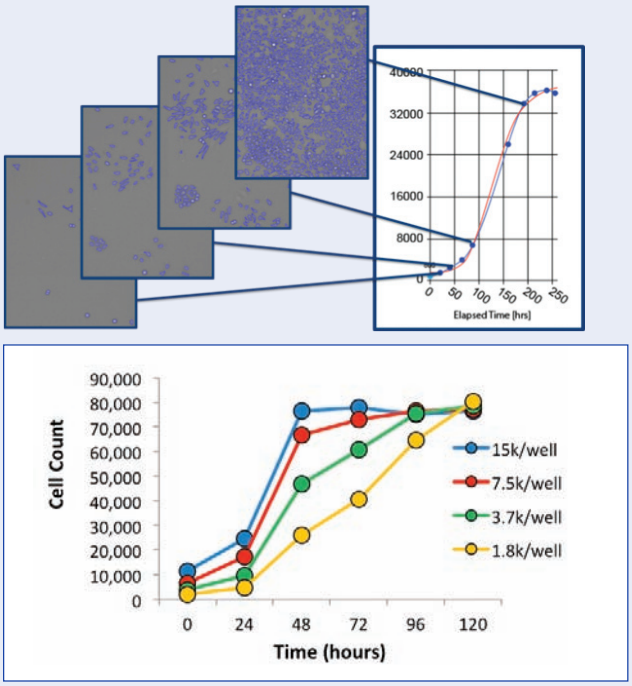

Cell growth tracking using Celigo. *Growth curves for CHO (DUXB11) cells grown in 96 well plates over 120 hours. Cells were imaged and counted using the Celigo Cell Counting application.*

Method 2

The second method is to measure confluence of the cell colonies. This method is most universal and applicable to the majority of cell types without customization.

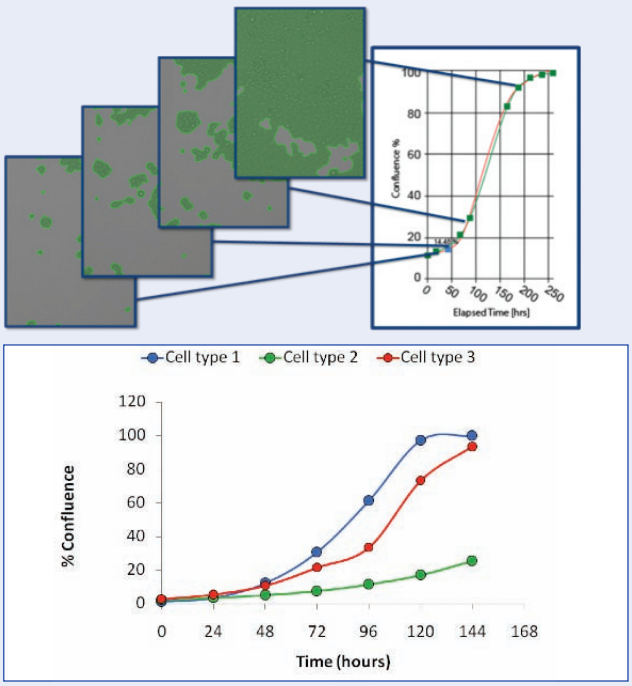

Streamlined cell culture maintenance using Celigo. *Example of workflow and output for monitoring adherent cell cultures in 96 well plates. Cells can be imaged and counted in culture vessels without staining or harvesting. Celigo updates and returns growth curves automatically.*

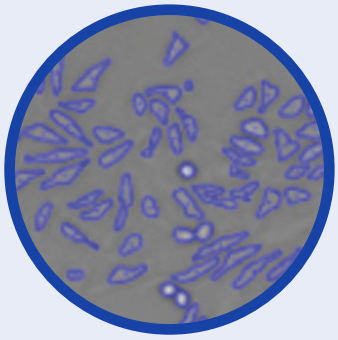

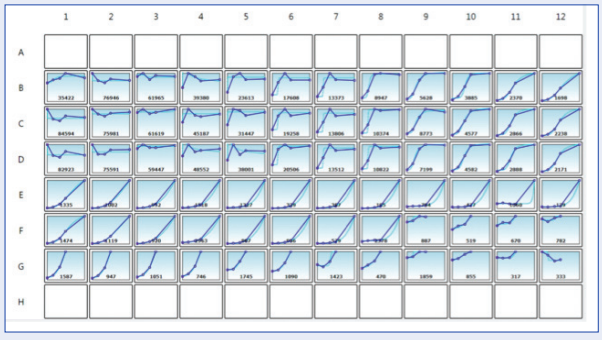

Cell growth curves are displayed in a 96-well plate.

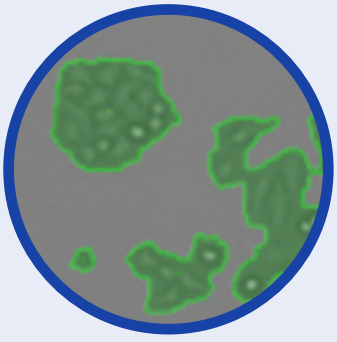

Morphology Screen of Toxic Compounds

A mixture of adherent and suspension cells were seeded into a 96-well plate. Using the Celigo gating interphase we can identify two distinct populations using morphology only. Designed to produce the enhanced bright field cell image, in combination with the advance image analysis software, Celigo has been used to identify, characterize and monitor specific cell sub-populations based on morphological features.

Celigo imaging cytometer records cell images, displays gated cell images, calculates cell morphological parameters and plots the data for population gating.

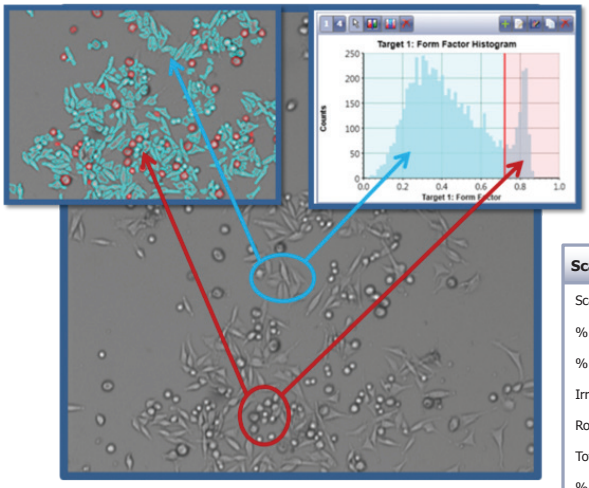

Scan Area Results	
Scan Area Location:	C5
% irregular:	83.15%
% round:	16.85%
Irregular Count:	5272
Round Count:	1068
Total Count:	6340
% Well Sampled:	100.00%
Average Target 1 Mean Intensity	105.69
Standard Deviation of Target 1 Mean Intensity:	34.54
Average Target 1 Integrated Intensity:	38,448.15

Control 48 hr

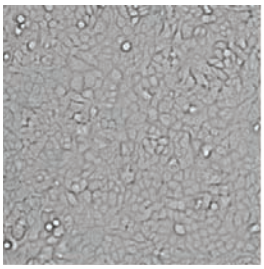

Camptothecin 48 hr

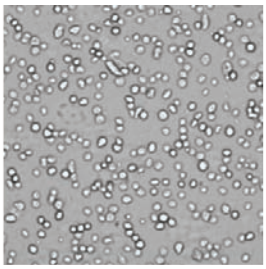

Alteration in cellular morphology was used as an indicator of compound toxicity. Above we can observe an example of the rounding up of an adherent cell after 48 hrs treatment with Camptothecin. Using this alteration in morphology in a label-free assay, we screened a number of compounds. Below you can observe the % survival index calculated from this assay.

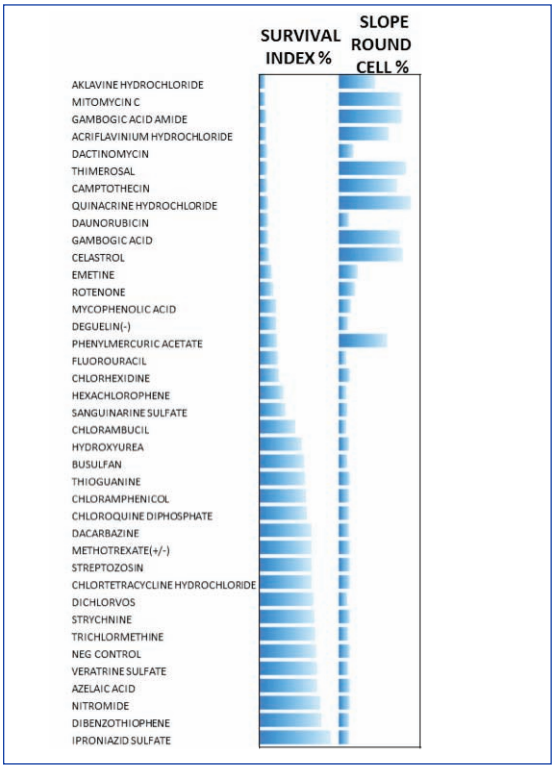

Cytotoxicity Assay for Drug Screening

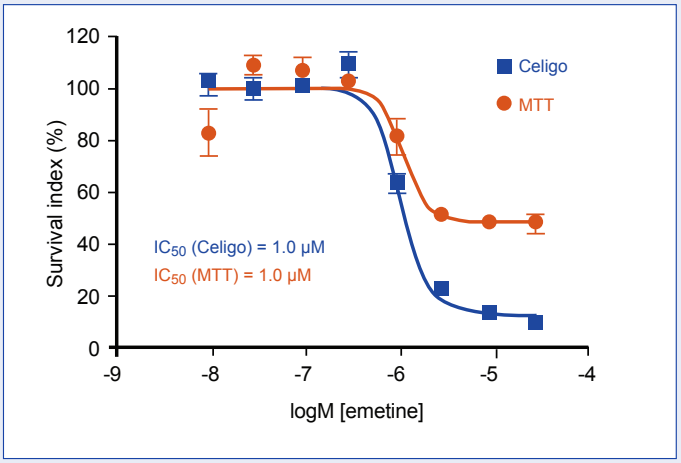

Dose-responses measured with the Celigo Cytometer versus MTT assay.
HL-60 and A549 cells were treated with compounds from 1 nM to 30 µM.

Automated Cytopathic Effect (CPE) Assay

Celigo imaging cytometer has been applied to provide automated, rapid assessment of viral infectivity in a range of microtiter plate formats. Using f-theta optics, Celigo provides high quality, whole well images using brightfield illumination. Automated segmentation and analysis provides quantitative output of CPE based on characteristic changes to the host cell monolayer.

- Objective segmentation and quantitative output of magnitude of infection
- Automated sample analysis reduces time, labor and variability
- High throughput and scaleable – less than 10 min for 96- or 384-well plate
- Capture high resolution, whole well images for documentation, audit trail or manual assessment of CPE
- Supports related fluorescent based functional assays relevant to infectivity (e.g. expression analysis, apoptosis)

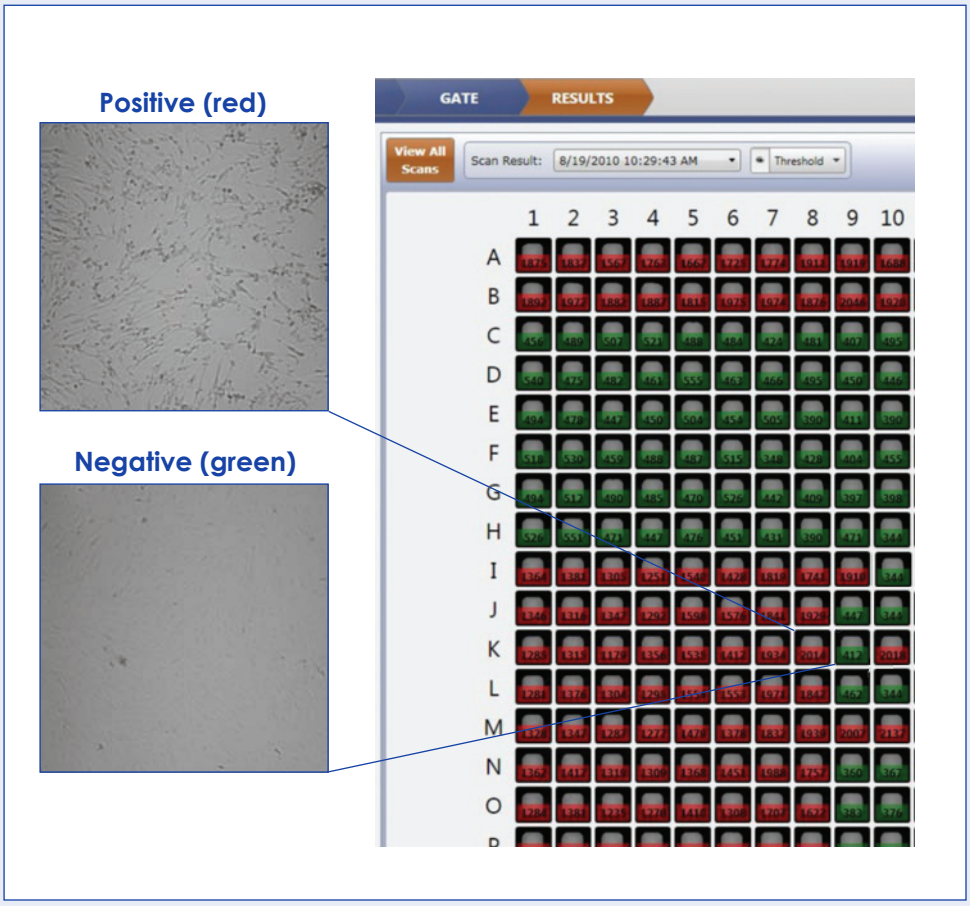

Bovine Viral Diarrhea (BVD) infection of Bovine Turbinate cells (BT2). Viral inoculum was serially diluted across the plate. Threshold function indicates red wells (infected) vs. green wells (uninfected). Celigo results demonstrate 100% correlation with manual CPE assessment via light microscopy

Wound Healing Assay

Celigo imaging cytometer has been applied to provide automated, rapid assessment of wound healing using the Oris Platypus plate technology. Automated segmentation of cells or confluency in both bright field and fluorescence is able to provide a quantitative output of wound healing / migration.

A. Wound Area Fill View

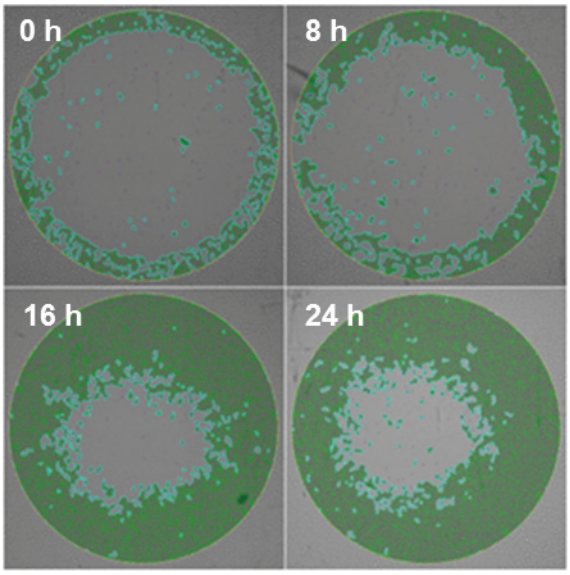

B. Dose-Response Curve

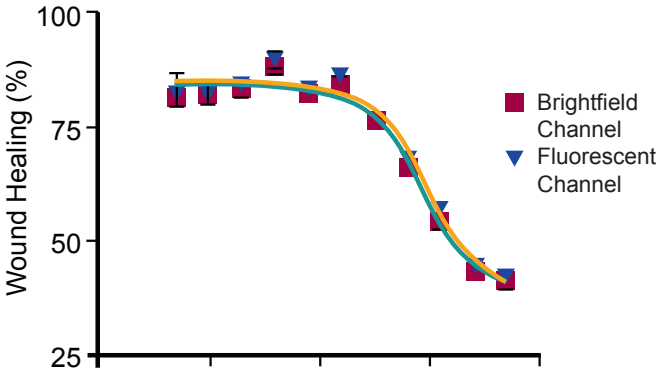

	BF Texture %wh	FL Texture %WH
EC50	8.064e-007	9.201e-007

Dose-response of % wound healing measured with the Celigo Cytometer using bright field and fluorescence.
(A)Wound area fill view at 0, 8, 16 and 24 hours. Confluence detection of the area covered within the wound is followed over time and a pseudo color green fill mask is added to aid visualization.
(B) HT1080 cells were plated in a 96-well Oris plate and allowed to grow to confluency. Upon removal of the plug the cells were treated with a dose response of Cytochalsin D and the confluence readout was read in bright field or in fluorescence after staining with Cell Tracker Green .

Cellometer® Simply Counted | Celigo® S Image Cytometer

www.nexcelom.com/celigo

Celigo® S

Monitor iPSC Reprogramming, Stem Cell Pluripotency, Differentiation

Here we demonstrate the ability of the Celigo adherent cell cytometer to combine the advantages of microscope imaging and flow cytometry population analysis in a plate-based kinetic assay for the study of iPSC reprogramming.

- Follow iPSC reprogramming over time without trypsinization
- Image, record and detect all the colonies in the whole well of 6-well plates
- Faster assay (7 minutes to read a 6-well plate)
- High proliferation rate of iPSC and death of feeder cell will not affect results as compared to FC analysis.

Using a transgenic MEF cell line containing mOrange OKSM and GFP Nanog we were able to track the evolution of iPSC colonies by detecting the production of orange colonies and the subsequent evolution of green colonies.

Monitor Murine Fibroblasts Reprogramming Over Time

iPSC Reprogramming Experiment 1

1. Plate at 5x 10^4 transgenic murine embryonic fibroblast (TMef) and 1x10^5 Wild-type (WTMef) in 6-well gelatin coated costar plate (cat # 3516).
2. Doxycyline induction of Yamanaka factors produce mOrange colonies and upon preprogramming progression colonies start to express Nanog GFP. Media is replenished every two days and contains Doxycyline to keep reprogramming on track. Nanog GFP normally appears at D8 so that is when imaging and colony counting starts.
3. To monitor the progression of reprogramming, the plates were scanned and analyzed to score total colonies and green colonies every two days from day 2 – day14.

Data courtesy of Kaji Lab, MRC Centre for Regenerative Medicine, University of Edinburgh.

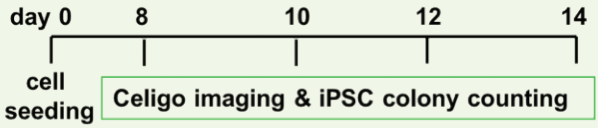

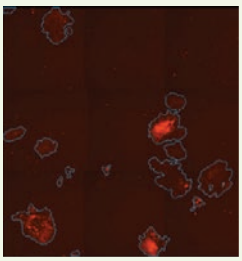

Count mOrange+ colonies

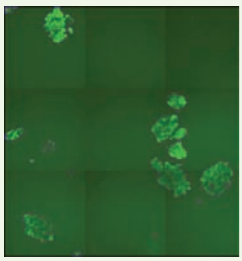

Count Nanog GFP

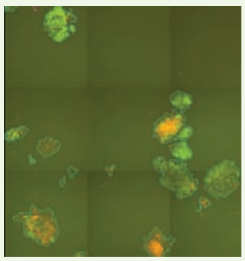

Overlay of green and red images

Level of Reprogramming

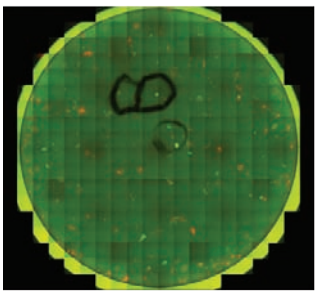

Low

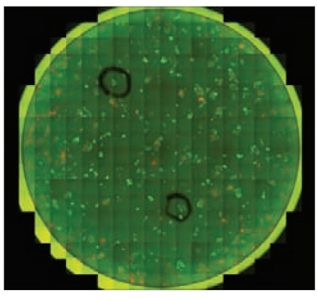

High

Reprogramming	# of Colonies	# of Orange Colonies	# of Green Colonies	% Reprogramming
Low	200	200	50	25
High	700	700	600	86

iPSC Reprogramming Experiment 2

The Celigo assay allows researchers to investigate other factors involved in the reprogramming process. Here we can observe that the addition of shRNA for factor x enhances the production of Nanog-expressing colonies. From this data we can summarize that factor x acts upstream of OKSM and downstream of Nanog and may play a key role in iPSC reprogramming

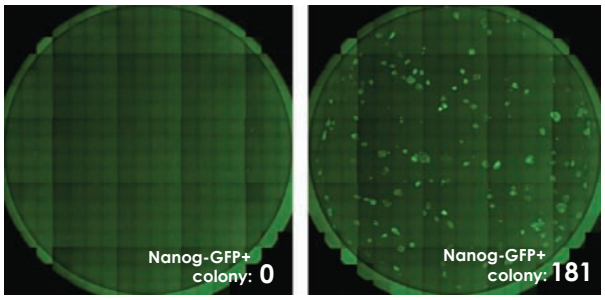

Current practice in iPSC Reprogramming Analysis

A combination of microscope and flow cytometry analysis were used. The microscope was used to visualize reprogramming. One or two representative colonies were manually chosen to image throughout the process. iPSC antigen expression was then examined using flow cytometry post-trypsinization.

Disadvantages of Microscope Analysis for iPSC Reprogramming

- Can only follow a small number of colonies throughout the reprogramming
- Colonies chosen to follow the reprogramming process may not be ideal examples
- Finding the same focal plane not always possible
- Images need to be exported and analyzed on a separate image processing software package.

Disadvantages of Flowcytometer Analysis for iPSC Reprogramming

- Trypsinize stem cell colonies into single cell suspension for cell population analysis does not reflect colonies with varying size and composition
- Interference from MEF cells and dead cells due to trypsinization and manipulation
- Destructive, requiring new sample for each time point

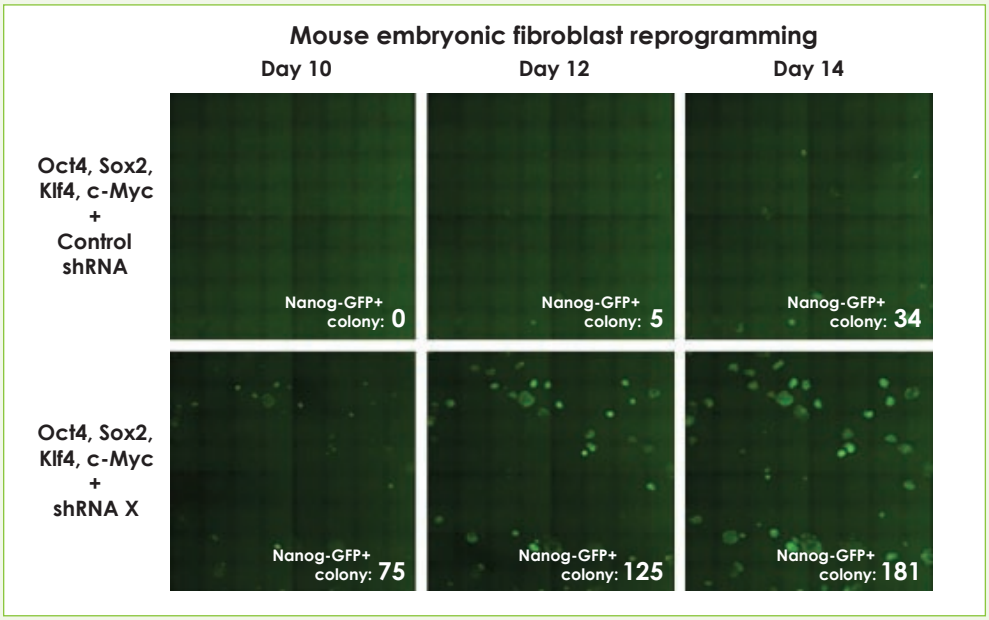

Monitor Human Fibroblasts Reprogramming Over Time

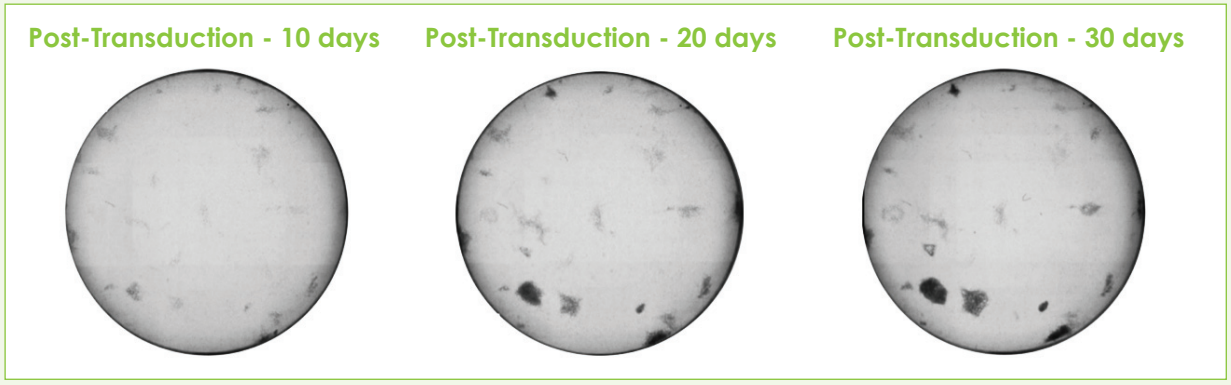

Whole-well imaging of human fibroblasts reprogramming experiments monitored in 12-well plates using the Celigo at 10 and 30 days post-transduction.

Measure Stem Cell Pluripotency with Live-Cell Staining

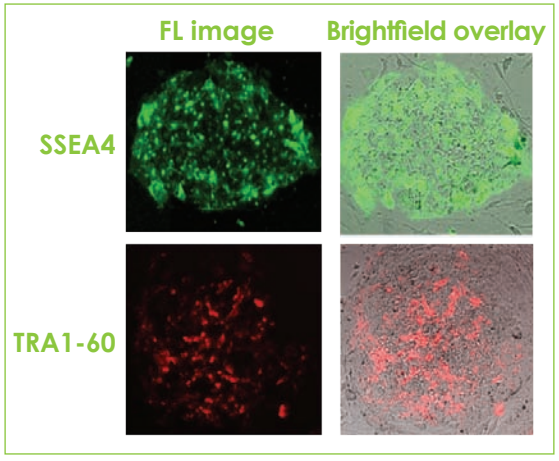

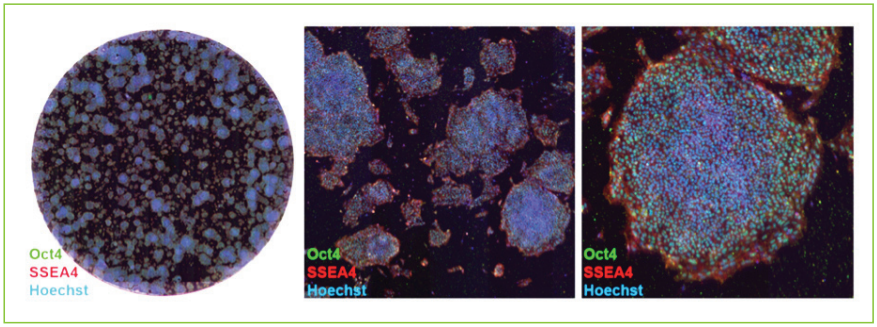

www.nexcelom.com/celigo

Multiplex Fluorescence Assays for Adherent Cells without Trypsinization

The combination of a bright field and three fluorescent channels allows the Celigo to perform many multiplexed assays. A gating interface similar to flow cytometry provides great flexibility in data analysis. In addition, images of gated cells are displayed and updated with the gating operation.

- Reduce sample preparation and number of cells per test (96 or 384 wells)
- Cells stay in multi-well plates without trypsinization
- Images provide visualization of cell morphology, fluorescent distribution for assay development and quality control
- Gating is reflected on cell images

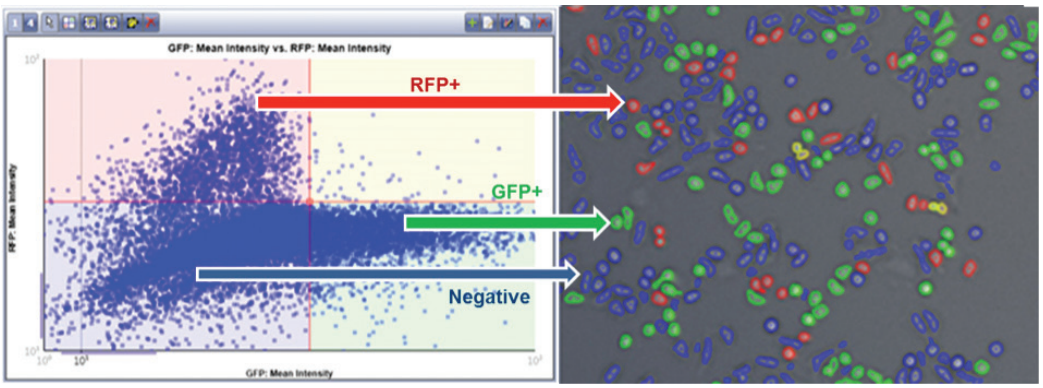

Fluorescence Proteins

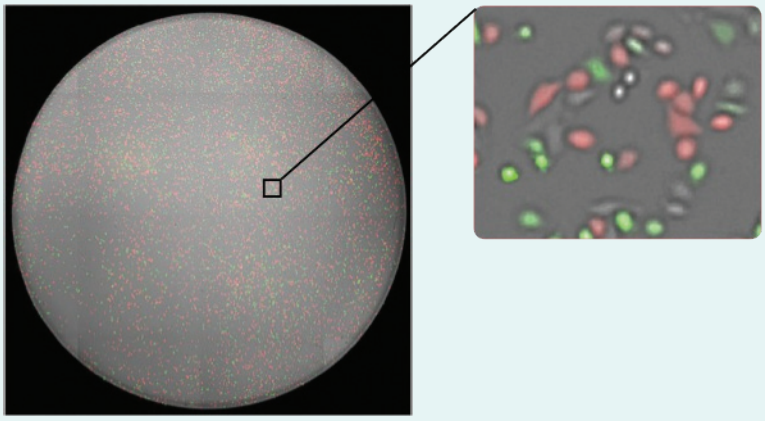

Whole well view GFP/RFP transfected Hela cells in a 96-well plate.

- Identify cells in bright field image
- Measure fluorescent protein signals in green, and red channels
- Label-free, non-invasive – no need to trypinsize adherence cells
- Quantify fluorescent protein signals on a cell-by-cell basis continuously on the same plate providing temporal data.
- Add propidium iodide for viability of GFP transfected cells in the same well

Transfection and Transduction Optimization using Celigo Adherent Cell Cytometer

The combination of a bright field and three fluorescent channels allows the Celigo to perform many multiplexed assays. A gating interface similar to flow cytometry provides great flexibility in data analysis. In addition, images of gated cells are displayed and updated with the gating operation.

Example 1. GFP Transfection Optimization in 96 Well Plates Without Trypinization

HeLa cells were transfected with a range of plasmid concentrations encoding turbo-GFP1 and seeded into a 96-well plate. To monitor cell death, propidium iodide was added to the wells in some experiments. The same plate was imaged daily over a 5-day period.

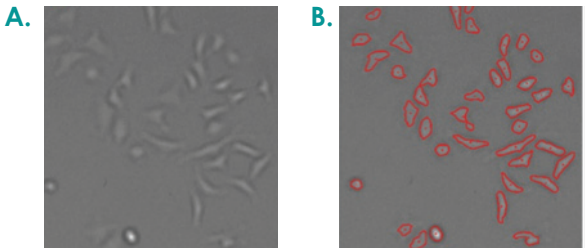

Figure 1. Cell Images of GFP transfected HeLa in 96-well plate. (A) Bright field cell image including transfected and non-transfected cells. (B) Celigo image process software identifies all the cells using bright field image, indicated by the red outline. (C), (D) Within this red outline, green fluorescence intensity was measured to gate cell populations and produce transfection efficiency.

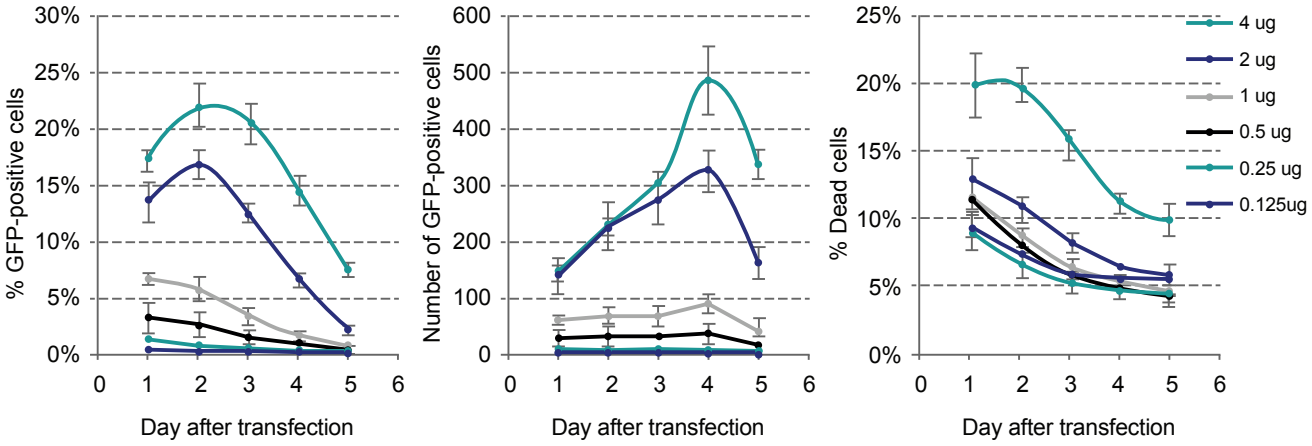

Figure 2. GFP-Positive Cell Quantification. Left: Percentage of GFP-positive cells vs. day after transfection. Middle: GFP-positive cell counts. Right: Percentage of dead cells (propidium iodide-positive). Error bars indicate standard deviation.

Example 2. Measure % RFP Positive Cells in Samples Containing GFP, RFP and Non-Expressing Cells

96-well containing samples with varied % of RFP, GFP and non-expressing HeLa cells were counted using Celigo. Bright field, green fluorescence and red fluorescence channels were used.

Step 1. Acquire & View Images on Celigo Image Cytometer

Bright field image of well D6, zoomed view.

RFP fluorescence image of well D6, zoomed view.

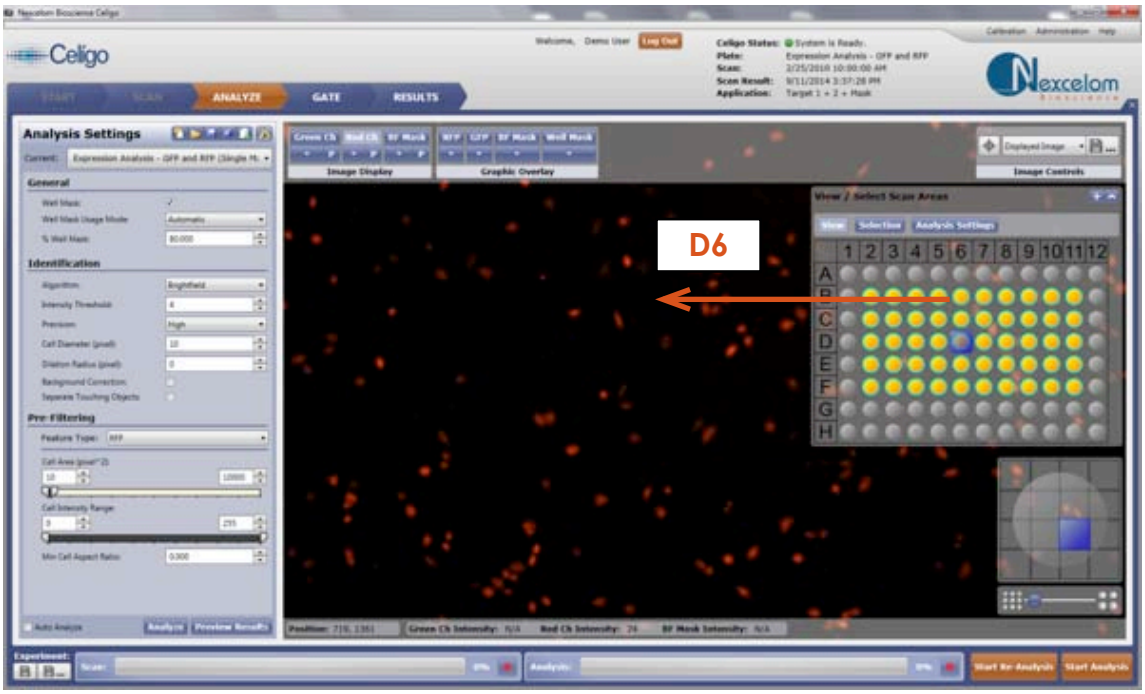

Step 2. Gate and Circle Counted Cells Automatically

Overlay of bright field, GFP+ and RFP+ cells identified by Celigo image processing software. GFP vs RFP intensity scatter plot is also shown. When the gate on the scatter plot is modified by dragging, the counted cell image is updated automatically.

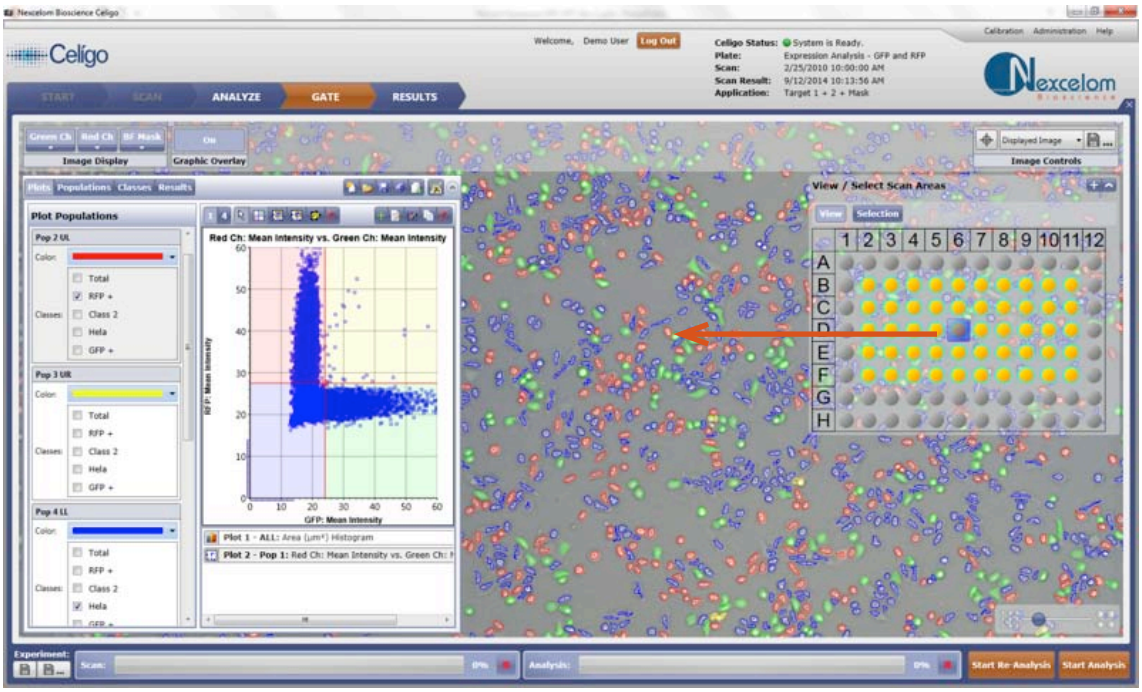

View whole well cell images

Double click any well on the well map to display whole well images. Zoom in to see details as listed in Table 1.

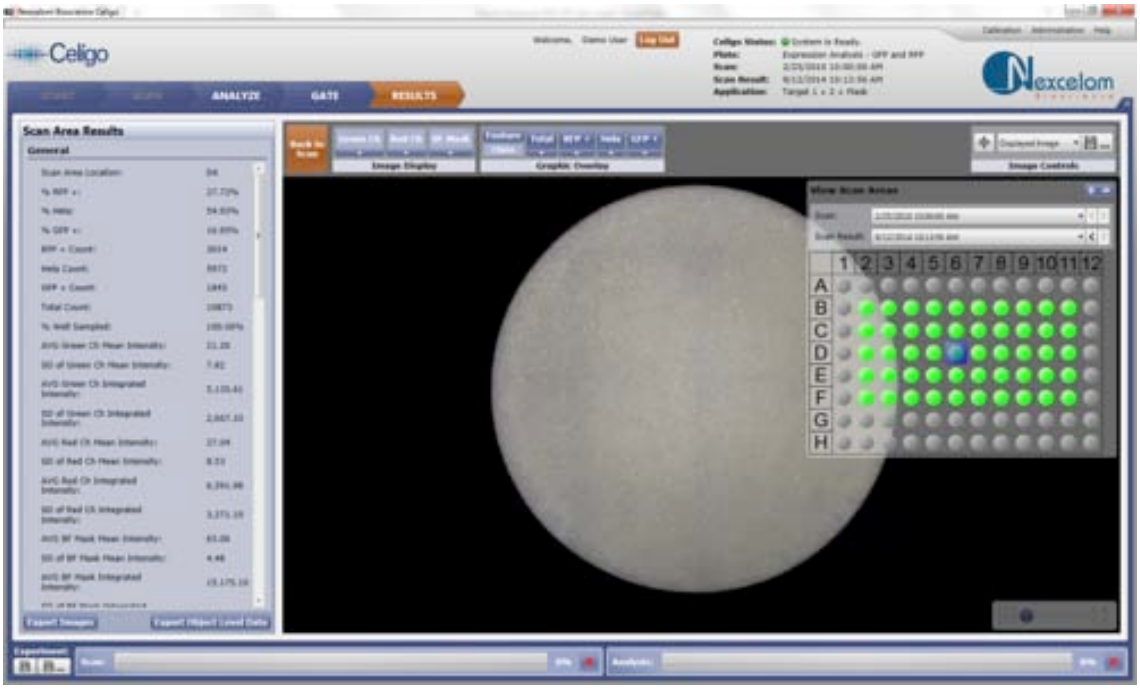

Table 1. Cell image examples from wells with varied RFP+ cell populations.

Cell Images		
GFP+, RFP+, GFP-RFP-	RFP+	Counted RFP+
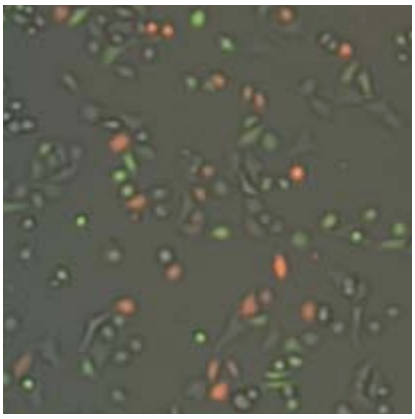	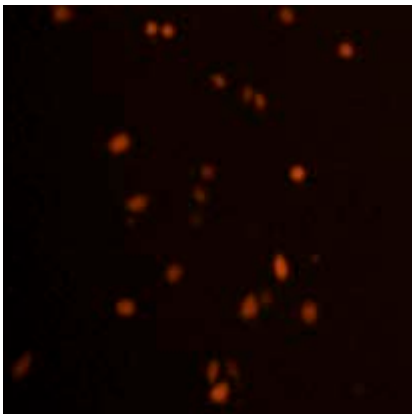	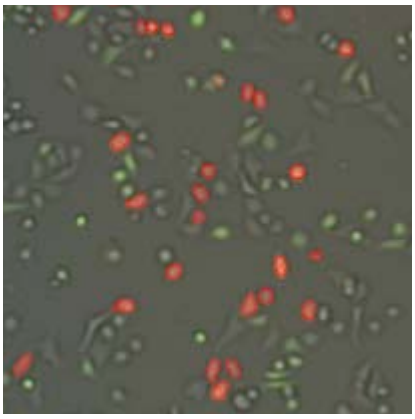
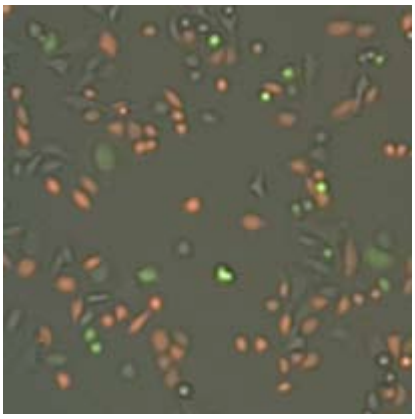	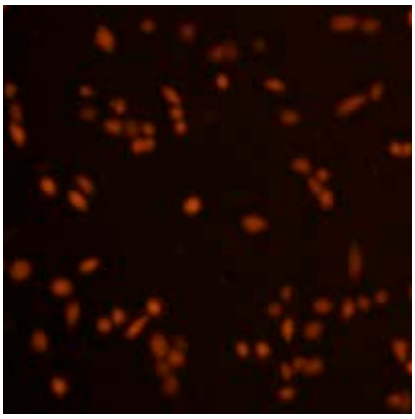	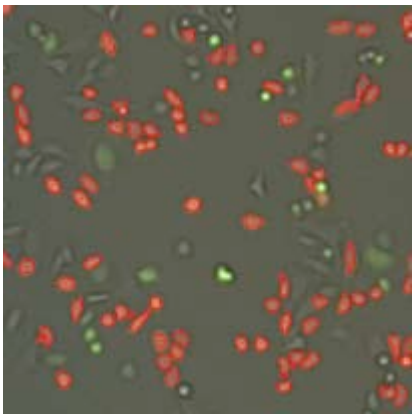
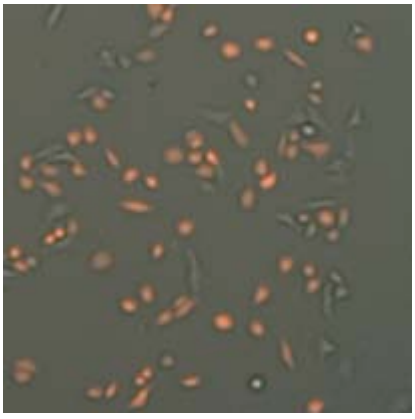	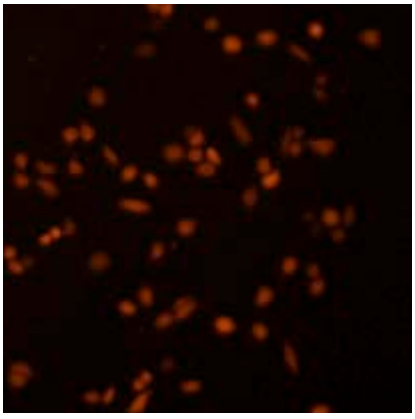	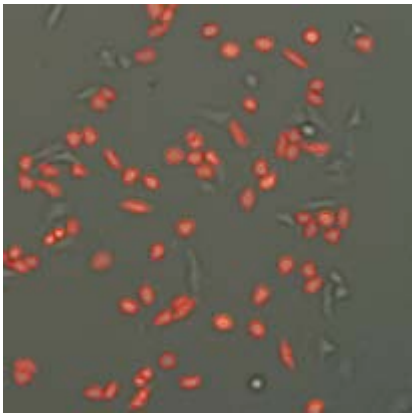

Step 3. Review Plate Level Results for Each of the Wells in the 96-Well Plate

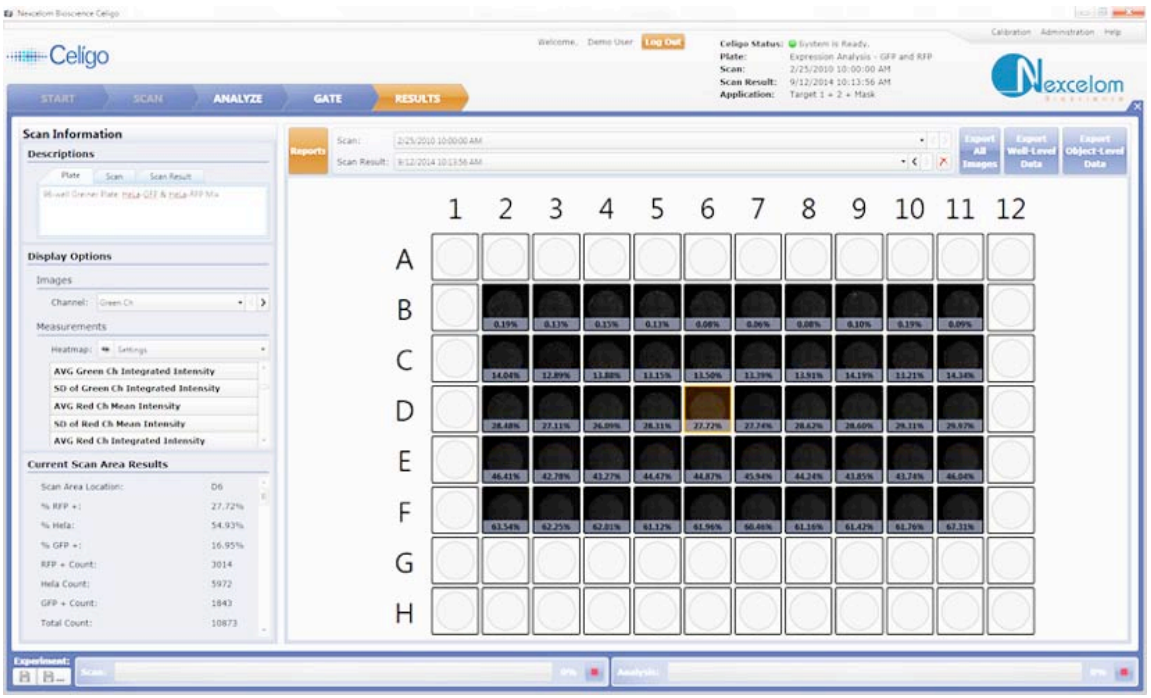

Reported Data	%	Count	Mean Intensity AVE & SD	Integrated Intensty AVE & SD
Total		•		
RFP+	•	•	•	•
GFP+	•	•	•	•
Non-FL HeLa	•	•	•	•
Green Channel			•	•
Red Channel			•	•
Brightfield Mask Channel			•	•

More plots are available from Celigo software, as listed in Table 2.

Table 2. Example plots

GFP vs. RFP Scatter Plot	RFP Intensity Histogram
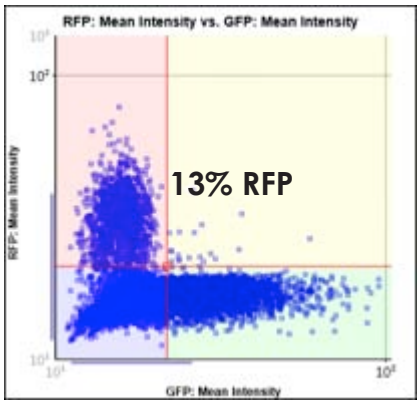	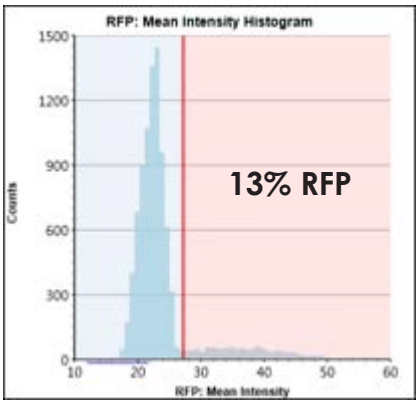
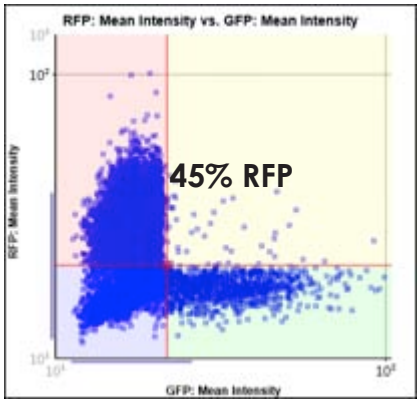	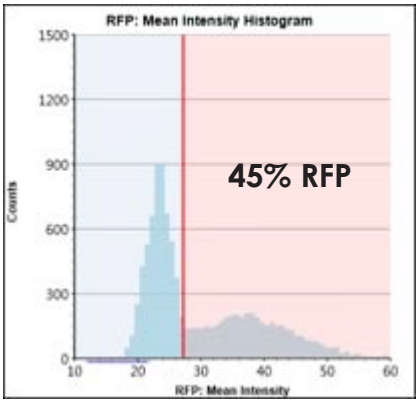
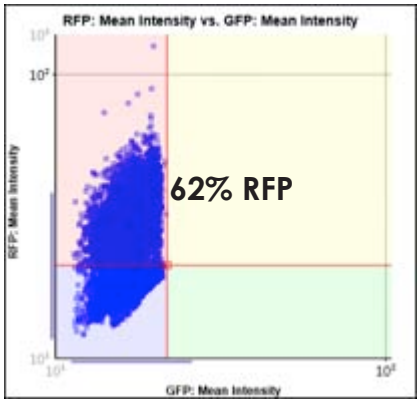	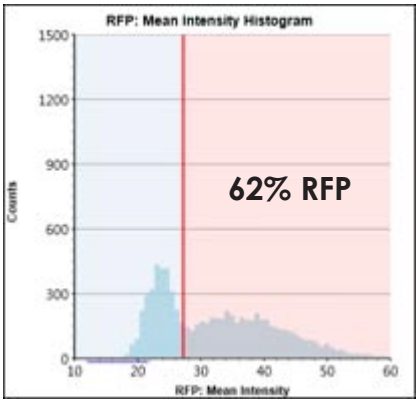

Step 4. Export Results for Each of the Wells in the 96-Well Plate and Produce Data Plot

Open Well Level Data in Excel / Calculate AVE & SD / Create Plot with Ave & Std

Measurement Plate Maps

% RFP +	1	2	3	4	5	6	7	8	9	10	11	12	% RFP +	
A													AVE	SD
B		0.2%	0.1%	0.1%	0.1%	0.1%	0.1%	0.1%	0.1%	0.2%	0.1%		0%	0%
C		14.0%	12.9%	13.9%	13.2%	13.5%	13.4%	13.9%	14.2%	13.2%	14.3%		14%	0%
D		28.5%	27.1%	26.1%	28.3%	27.7%	27.7%	28.6%	28.6%	29.3%	30.0%		28%	1%
E		46.4%	42.8%	43.3%	44.5%	44.9%	45.9%	44.2%	43.8%	43.7%	46.0%		45%	1%
F		63.5%	62.3%	62.0%	61.1%	62.0%	60.5%	61.2%	61.4%	61.8%	67.3%		62%	2%
G														
H														

% Hela	1	2	3	4	5	6	7	8	9	10	11	12	% Hela	
A													AVE	SD
B		62.1%	62.7%	63.0%	61.9%	64.4%	60.8%	61.4%	63.0%	61.1%	60.2%		62%	1%
C		61.0%	69.5%	58.6%	60.6%	58.8%	58.0%	58.5%	58.5%	58.4%	55.0%		60%	4%
D		53.8%	53.9%	55.1%	52.6%	54.9%	59.4%	51.6%	51.2%	51.6%	48.2%		53%	3%
E		44.1%	47.3%	46.2%	45.3%	45.2%	43.9%	45.2%	46.4%	46.9%	43.4%		45%	1%
F		36.3%	37.6%	37.8%	38.7%	37.8%	39.2%	38.3%	38.3%	37.7%	32.5%		37%	2%
G														
H														

% GFP +	1	2	3	4	5	6	7	8	9	10	11	12	% GFP +	
A													AVE	SD
B		37.4%	37.1%	36.7%	37.8%	35.3%	38.9%	38.3%	36.6%	38.5%	39.5%		38%	1%
C		24.7%	17.3%	26.9%	25.9%	27.1%	28.1%	27.2%	26.9%	28.0%	29.8%		26%	3%
D		17.2%	18.3%	18.4%	18.6%	17.0%	12.5%	19.1%	19.6%	18.5%	21.0%		18%	2%
E		9.0%	9.4%	10.0%	9.7%	9.4%	9.6%	9.9%	9.3%	8.9%	9.5%		9%	0%
F		0.0%	0.0%	0.0%	0.0%	0.0%	0.0%	0.1%	0.0%	0.2%	0.0%		0%	0%

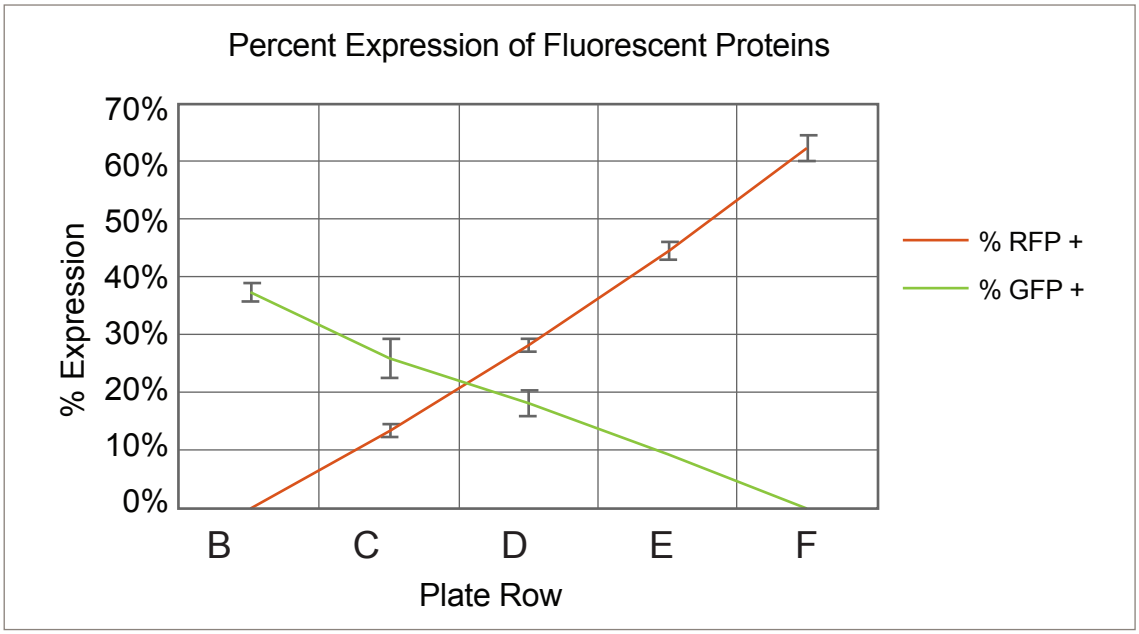

Cell Proliferation Assay Using BrdU Incorporation

Image Data

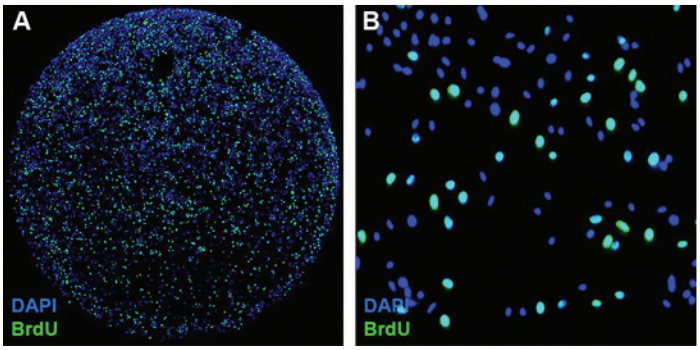

Gated Data

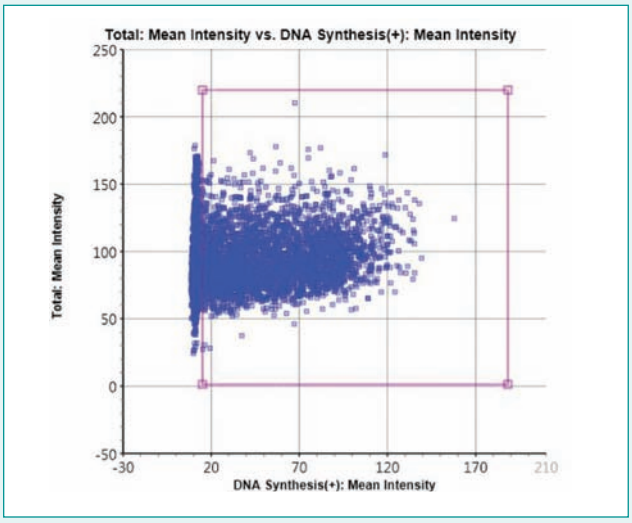

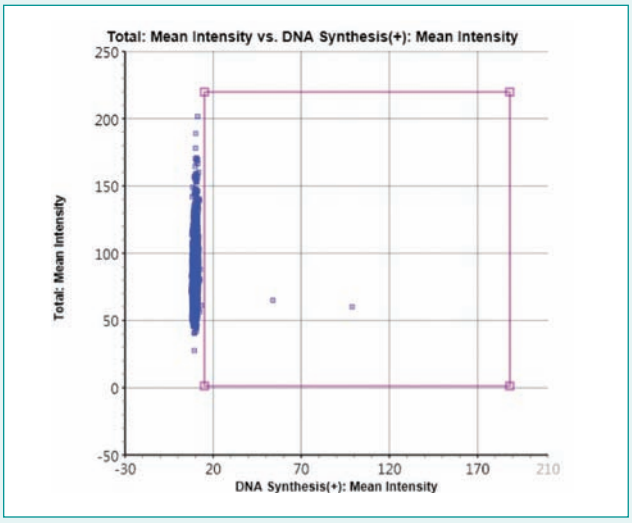

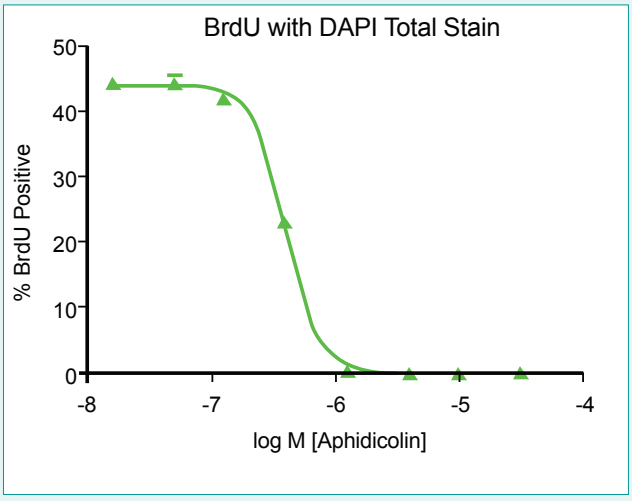

Cell Cycle Analysis of Adherence Cells in 96-Well Plates Using Celigo

Cells were stained with DAPI, a nucleic acid dye used for DNA content analysis. The multi-fluorescent channel analysis and gating interface allows identification of cells in the G0/G1, S-Phases and G2/M phases of the cell cycle.

Cell Cycle - Method 1: Measure DNA Content Using DAPI

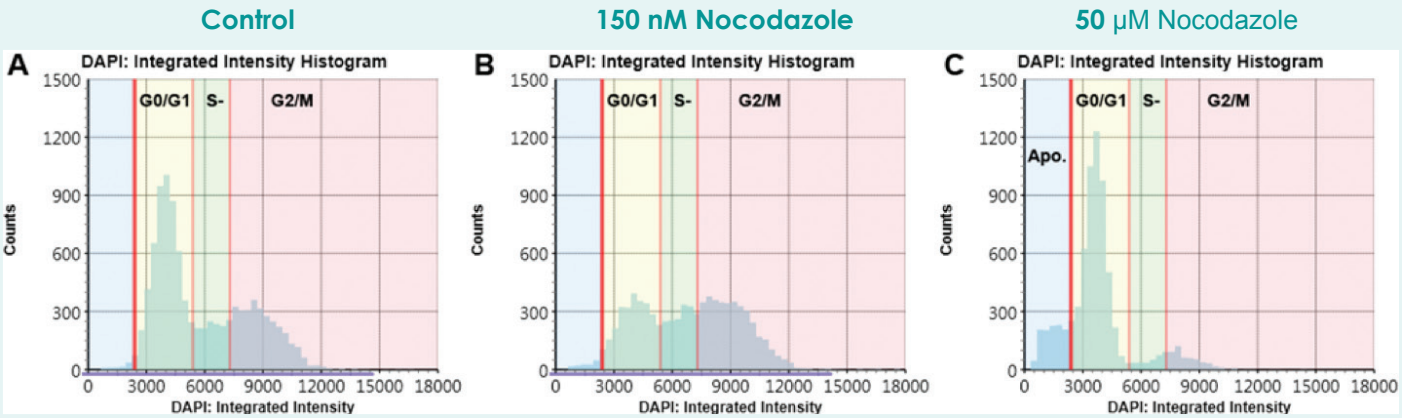

Cell Cycle-Method 2: Using DAPI and BrdU

- Cell cycle analysis is examined by measuring the amount of DNA per cell
- Incorporation of DAPI and BrdU
- Double peak characteristic peak of cell cycle consisting of G0/G1, S and G2/M phases

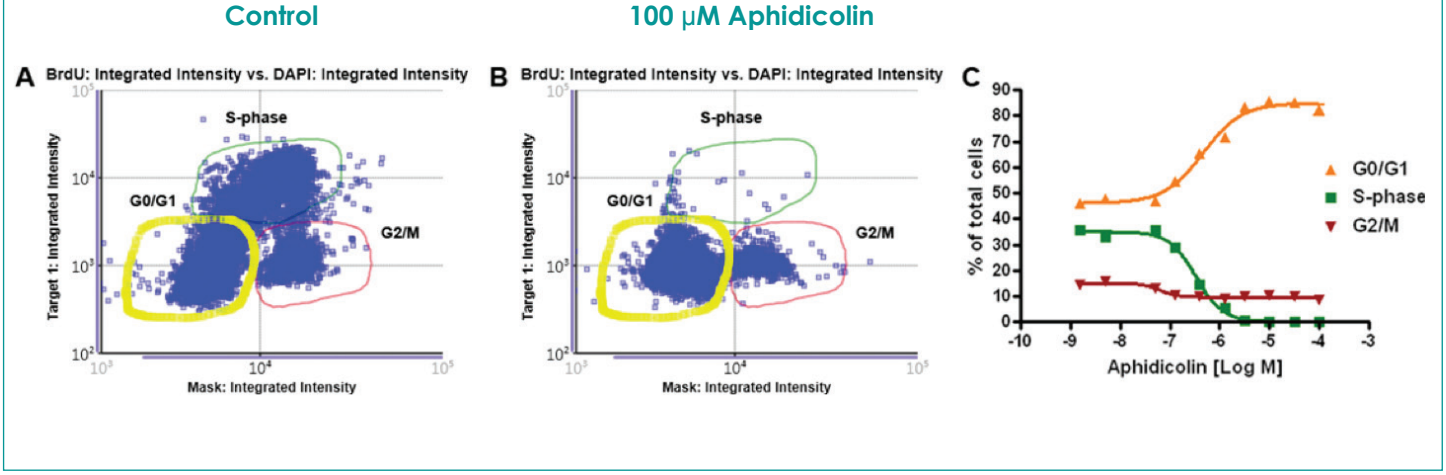

Imaging data can be used to generate dose response curves to characterize drug activities on the cell cycle (right panel).

Cell Viability Determined by Staining Cells with Live and Dead Cell-Specific Dyes

Briefly, cells are simultaneously stained with a mixture of calcein AM, propidium iodide, and Hoechst 33342 for respective staining of live, dead and all cells. Images are acquired and analyzed using the Celigo software. Markers are identified in each fluorescent channel and for each well of a microtiter plate, live and dead cell counts as well as the percentage of live and dead cells are automatically reported.

Cell Counting in 96-Well Plate

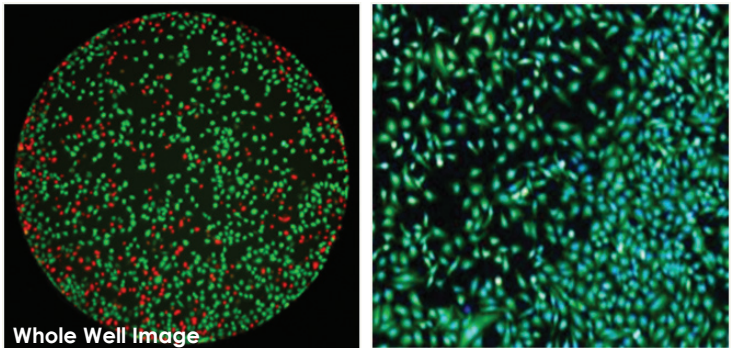

Green: Live, Dead: Red Green: Live, Blue: Total

Cell Cycle by BrdU

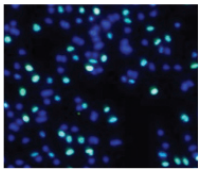

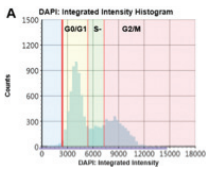

Apoptosis - PS Externalization

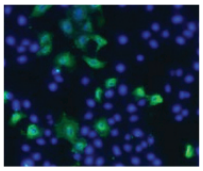

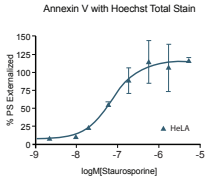

Cell Viability

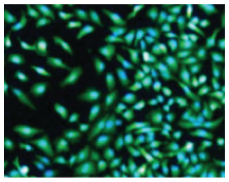

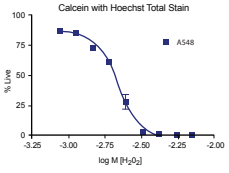

Transfection Efficiency

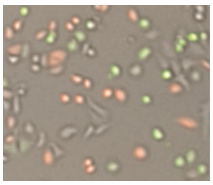

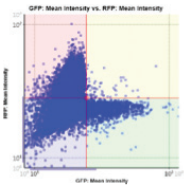

Migration

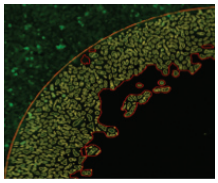

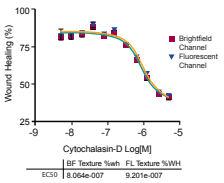

Viral Infection

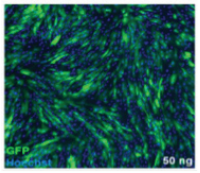

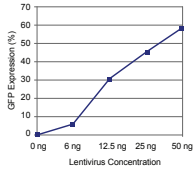

ERK Phosphorylation

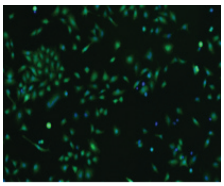

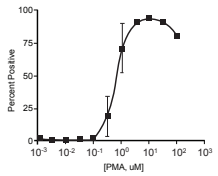

DNA Synthesis

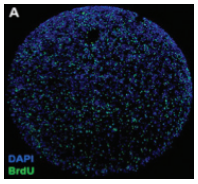

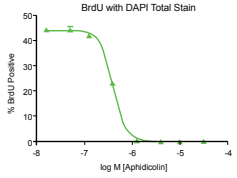

- Receptor internalization
- Phagocyosis
- Receptor detection: CD71, CD54 ICMA-1
- ERK Phophorylation
- Nuclear antigen detection

Cellometer® Simply Counted Celigo® Image Cytometer

www.nexcelom.com/celigo

Celigo® S

Cell Line Development – Single Cell Detection, Clonal Validation, Transfection

The process of developing a cell line to produce a specific protein or antibody involves multiple stages, all of which can be greatly aided by Celigo imaging cytometer.

Transfection
- Determine transfection efficiency
- Monitor stability of transfection

Stabilized Outgrowth
- Monitor growth in each well
- Identify confluent wells for passaging
- Increase growth with media optimization

Monoclonality
- Verify efficiency of limiting dilution, or single cell dispensing
- Identify single cell per well

Colony Outgrowth
- Confirm single colony

Robotic Integration

The Celigo provides an optional robotic API which can be controlled by various automation scheduling software applications. The Celigo is ready for integration with multiple automation partners and can be coupled with robotic arms, automated incubators and liquid handlers.

The Celigo can be used through the whole process of cell line development.

- Compatible with 96-, 384- and 1536- well plates.
- Identify wells with a single colony to avoid the time-consuming and manual identification of clones by eye.
- Measures colony size using bright field and aids the process of selecting wells for clonal expansion
- Automate cell line generation process with Celigo robotic integration.

Day 0 - Single Cell **Day 7 - Single Colony**

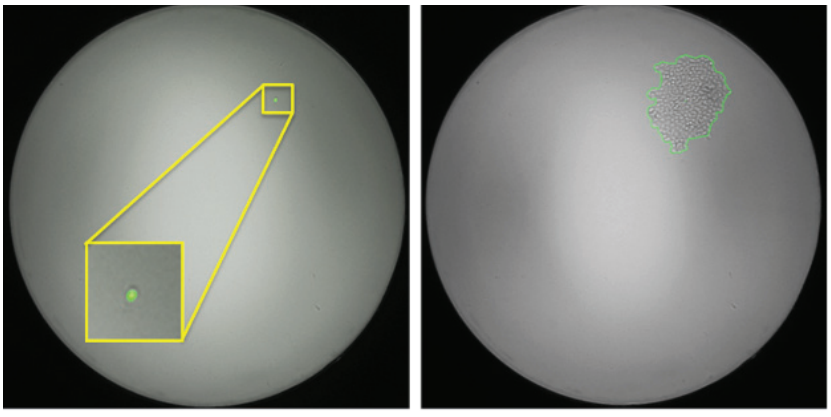

Well with Single cell that grew into a Single colony

Transfection & Transduction Optimization

- Quickly identify optimal parameters for high-efficiency transfection
- Determine transient and stable transfection rates and evaluate antibiotic induction using live imaging

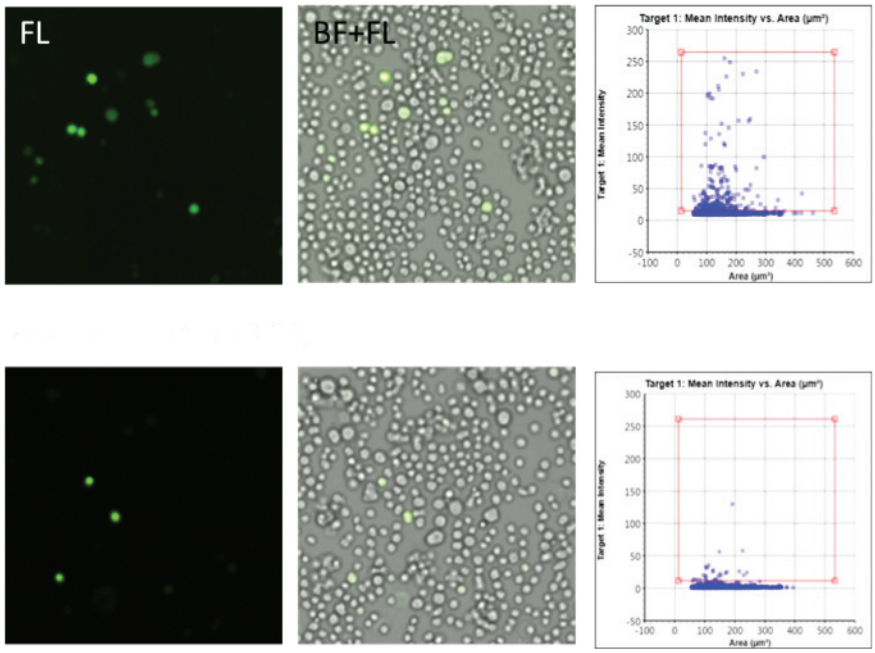

Sample 1 shows moderate transfection efficiency while sample 2 has lower efficiency.

- Monitor transfection efficiency on Celigo directly
- Acquire both bright field and green fluorescence cell images
- Identify all the cells using bright field
- Produce scatter plot for gating GFP+ cells
- Calculate % GFP+ cells automatically
- 96 or 384 wells

Cell Line Characterization

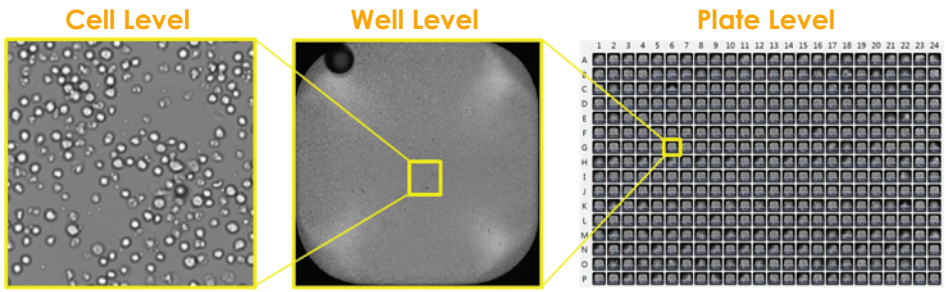

Brightfield images can be viewed from the cell, well or plate level.

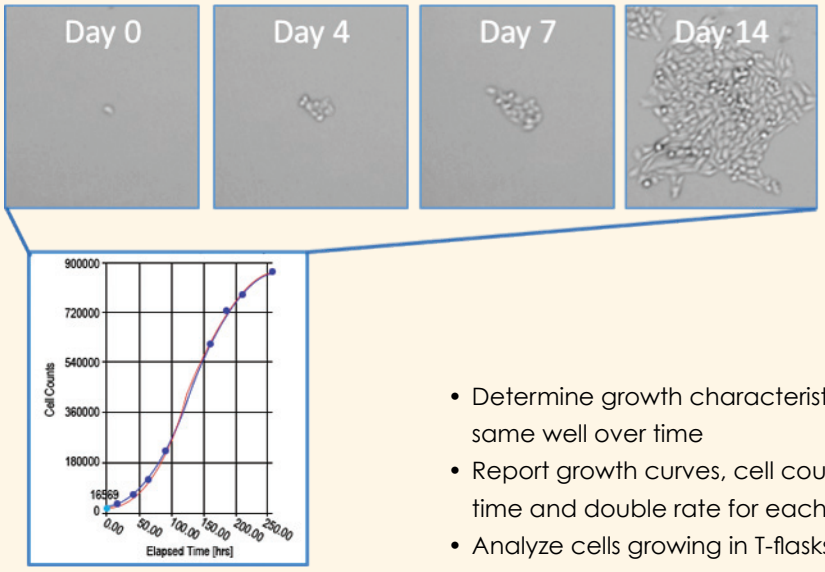

- Determine growth characteristics of cells directly from the same well over time
- Report growth curves, cell counts, confluence, doubling time and double rate for each well
- Analyze cells growing in T-flasks

Media optimization experiment using a single 384-well plate

- Providing additional nutrients to media can help increase proliferation rates.
- Evaluated media supplements using an 8-parameter design of experiment (DoE) methodology, where 3 reagents were mixed in multiple combinations.
- On day 0, 10 CHO-S per well were plated with supplement combinations using a 384-well plate, which allowed 35 replicates per condition.
- Three supplement reagents were tested on one 384-well plate for n=35 per condition

Monitoring Monoclonality and Outgrowth

Adherent Cells

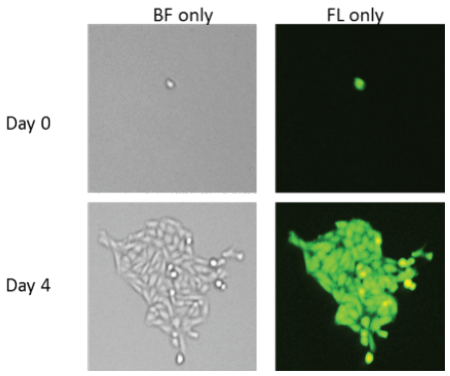

Suspension Cells

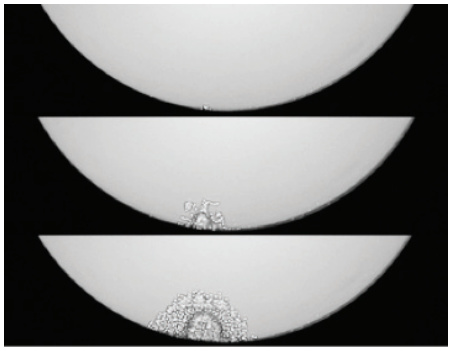

Dual channel bright field and fluorescent imaging of a single cell in a 96-well plate allows identification of candidate wells for clone development.

Single Colony BF Counts

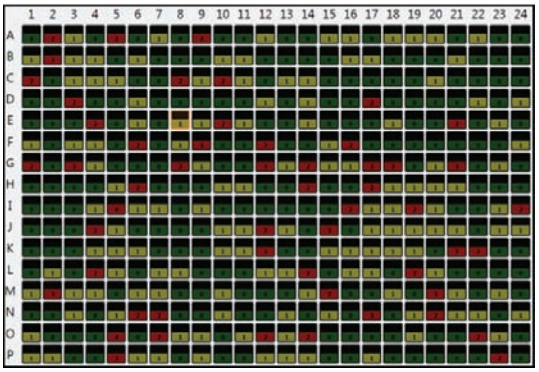

Single Colony FL Counts

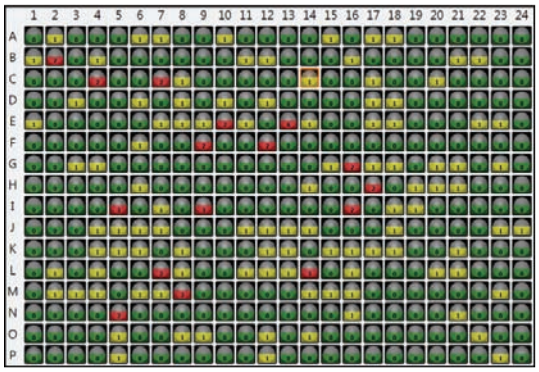

- Identify wells with single colony on the final day
- Identify wells with single cell on the first day
- Overlay single cell plate map with the single colony plate map to produce the heat map of single cell and single colony.

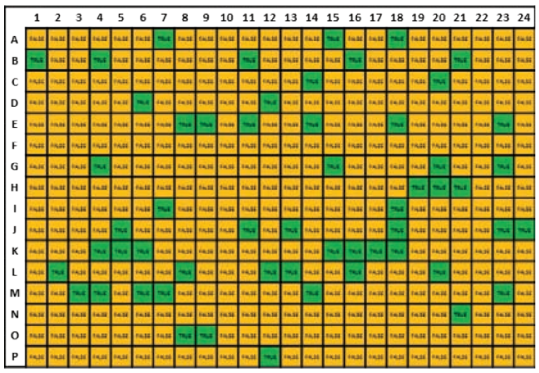

Cellometer® Simply Counted

Celigo® S Image Cytometer

Automated Imaging and Analysis of 3D Tumor Spheroids, Cancer Stem Cell Colony Formations

3D Tumor Spheroids Functional Assays

The Celigo imaging cytometer has been developed to fully automate imaging and analysis of tumorspheres, embryoid bodies and cancer stem cell colonies. It has been used in the development of 3D tumor spheroid-based functional assays for target validation and drug evaluation.

Data courtesy of Dr. Maria Vinci, Cancer Research UK, Cancer Therapeutics Unit, The Institute of Cancer Research.

Spheroid Generation

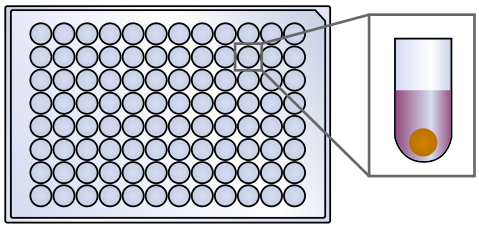

Ultra-low adhesion 96-well round bottom plate

Imaging

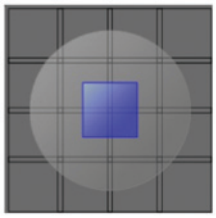

1/16 field of view per well

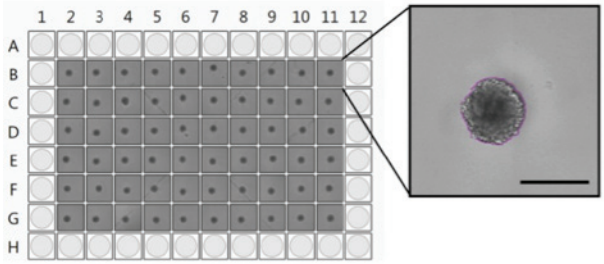

Spheroid Growth Curve

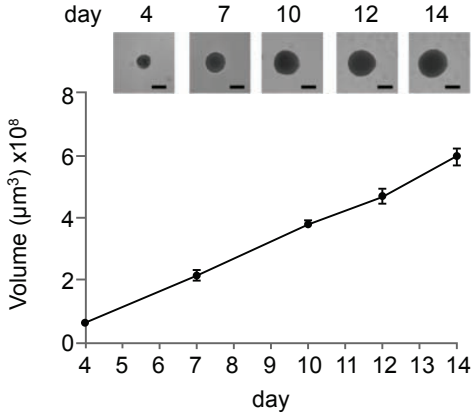

- Identify and count spheroids in flat or U-bottom wells.
- Eliminate cumbersome manual morphology measurements and improve data reproducibility.
- Monitor growth of spheroids over time.
- Screen numerous spheroid plates per day, 96, 384 well plates
- Scan an ultra-low adhesion 96-well plate in 8 minutes
- Measure viability using dual-fluorescence assays
- Multi-parameter analysis

Counts / Size / Short & Long Diameter / Est. Volume / Perimeter /Area / More ...

Tumor Spheroid Growth Inhibition Assay

4-day old spheroids were treated with compounds for 72 hours. Drug induced concentration-dependent growth inhibition was obtained.

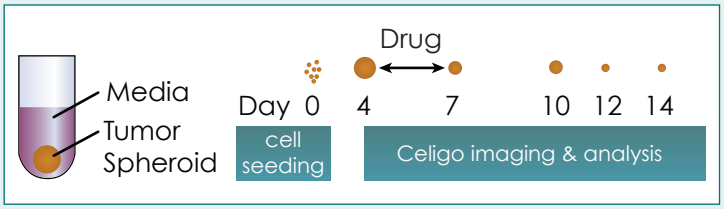

- Day 0 - 4: form spheroids
- Day 4 - 7: drug treatment
- Day 4 - 14: measure spheroid size

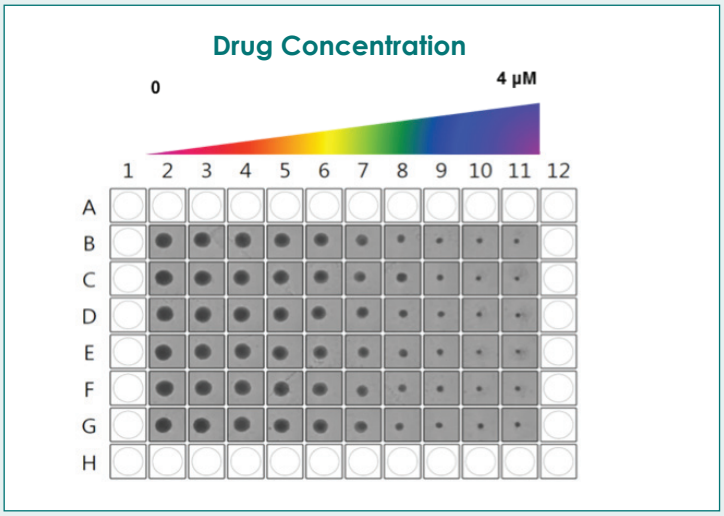

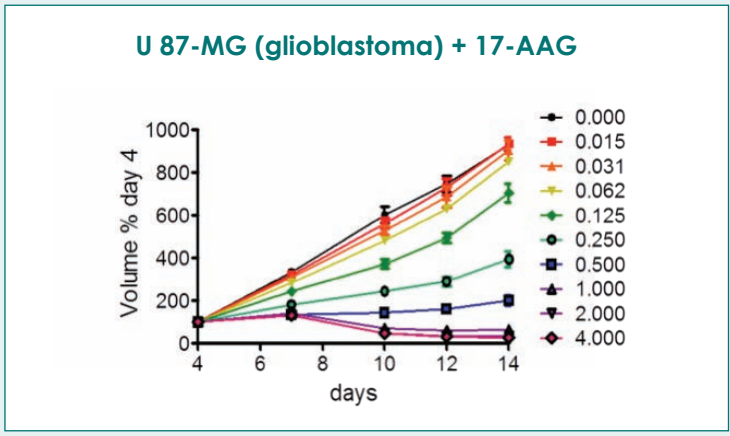

Vince et al. BMC Biology 2012, 10:29, March 2012

Invasion into Matrigel Assay

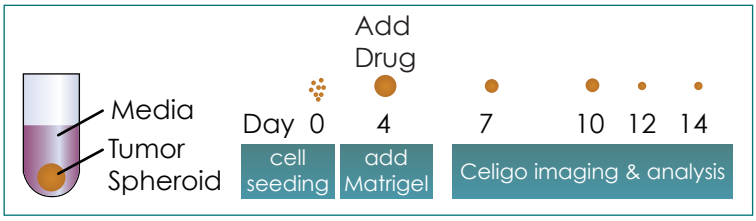

- Day 0-4: form spheroids
- Day 4: add Matrigel to provide a semi-solid gel-like matrix
- Day 4-7: use Celigo imaging cytometer to determine the area occupied by individual cells or cell clusters

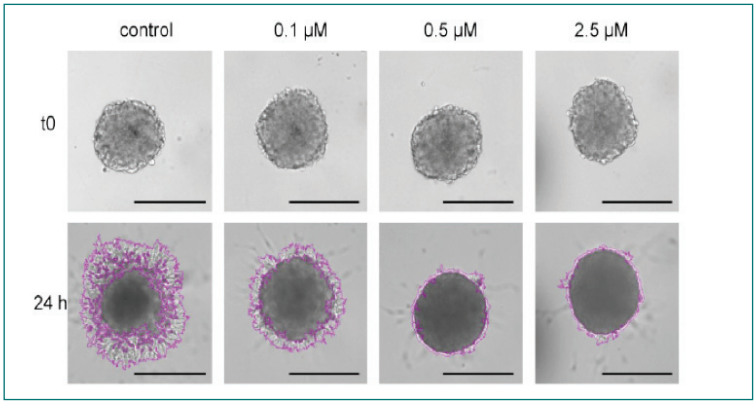

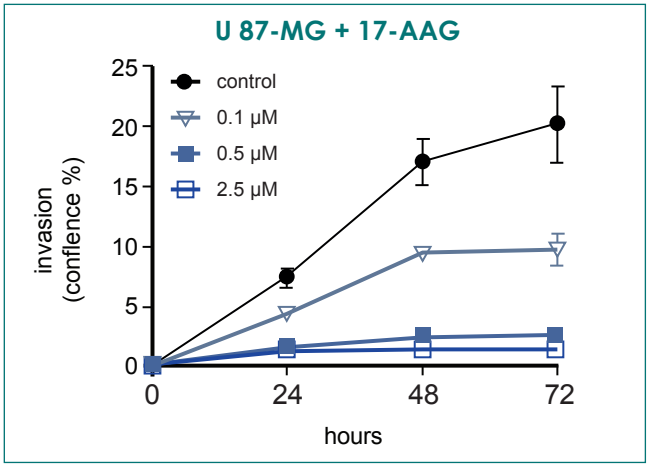

Two-Fluorescence Viability Assay for 3D Tumor Spheroids

3D cultures were treated with multiple drugs (17-AAG, Paclitaxel, TMZ or Doxorubicin) and stained for viability after 21 days.

Live / dead stains used were Calcein AM (green), Propidium Iodide (red) to measure live and dead cells on days 4, 7, 10, 14, and 17. Plates containing spheroids were imaged on Celigo imaging cytometer.

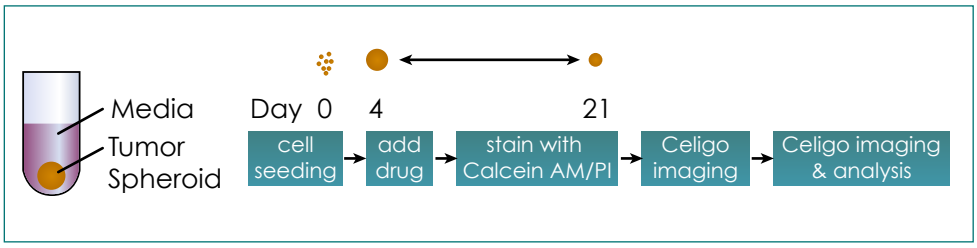

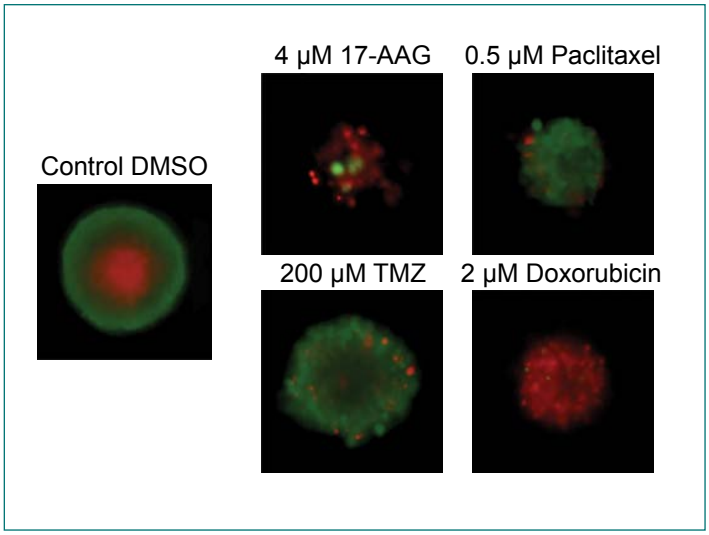

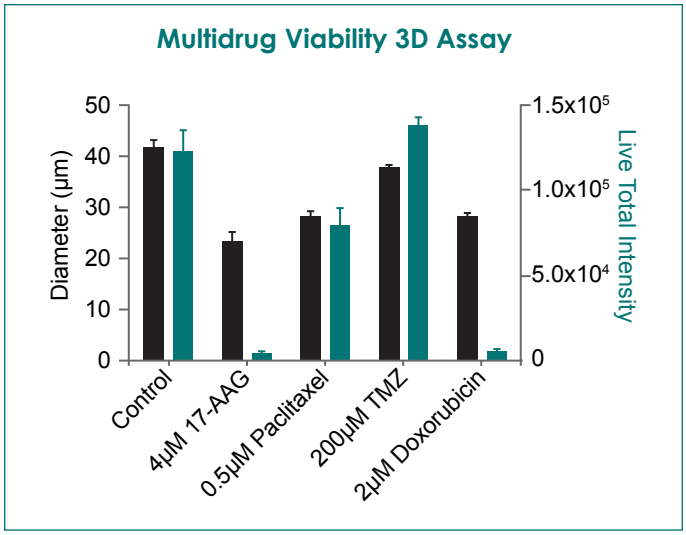

- 17-AAG decreased sphere size and caused the most significant cell death
- Paclitaxel decreased sphere size but maintained a signifiicant number of live cells
- Temozolomide caused no significant decrease in sphere size and did not cause cell death
- Doxorubicin decreased sphere size and caused significant cell death

Spheroid diameter (black) and total live fluorescent intensity (green) after drug treatment.

Tumorsphere Formation Assay

These assays utilize Celigo's brightfield imaging mode and multiple quantification methods to obtain number and size of tumorspheres cultured in 96, 48, 24, 12, and 6-well microplates, as well as 60mm dish.

MDA-MB-436 Spheroids

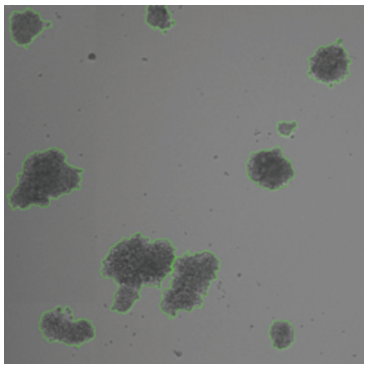

Zoomed view of SKBR3 Spheroids

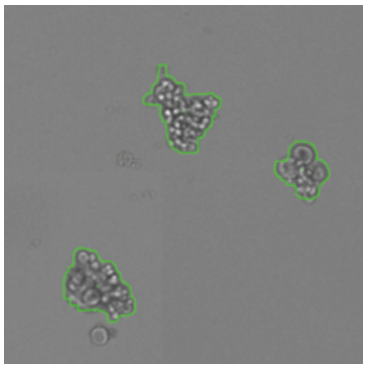

The green outlines indicate counted spheroids.

Cellometer® Simply Counted

Celigo® S Image Cytometer

Direct Cell Counting Assays for Immuno Therapy

Cytotoxicity assays play a central role in studying the function of immune effector cells such as cytolytic T lymphocytes (CTL) and natural killer (NK) cells. Traditionally, cytotoxicity assays have been performed using Chromium-51 (^{51}Cr) and Calcein release assays.

The assays involve labeling tumor cells (target) with radioisotope or fluorescent dyes, when the target cells are subjected to CTLs or NK cells (effector) mediated killing, they release the entrapped labels into the media. The amount of released label in the media is measured to determine the level of cytotoxicity the effectors have induced.

A novel cytotoxicity assay using the Celigo imaging cytometer to directly count live, fluorescently labeled target cells has recently been introduced.

Celigo Imaging Cytometry for Direct Cell Counting ADCC Assay

1. Celigo Imaging Cytometer is a plate-based cytometer that can scan the entire well of standard microplates and captures bright-field and fluorescent images.

2. The captured images are analyzed with the Celigo software to measure size, morphology, cell count, confluence, and fluorescent intensity.

3. The measured parameters are used to generate cell proliferation kinetic data, GFP/RFP expression, tumor spheroid size change, DNA cell cycle analysis, apoptosis, and ADCC cytotoxicity results.

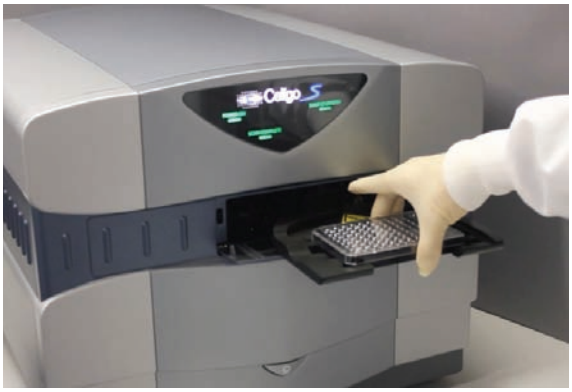

Direct Cell Counting Method using Calcein AM

- Uses Celigo to capture and analyze bright-field and green fluorescent images
- Target suspension and adherent cells are stained with Calcein AM and then mixed with the Effector cells
- The number of Target cells (Calcein+) are counted and monitored over time
- Reduction in Target cell number indicates cell-mediated or antibody- dependent cell-mediated cytotoxicity (ADCC)

4. Celigo image cytometer produces whole well images for 96-, 384-well plates.

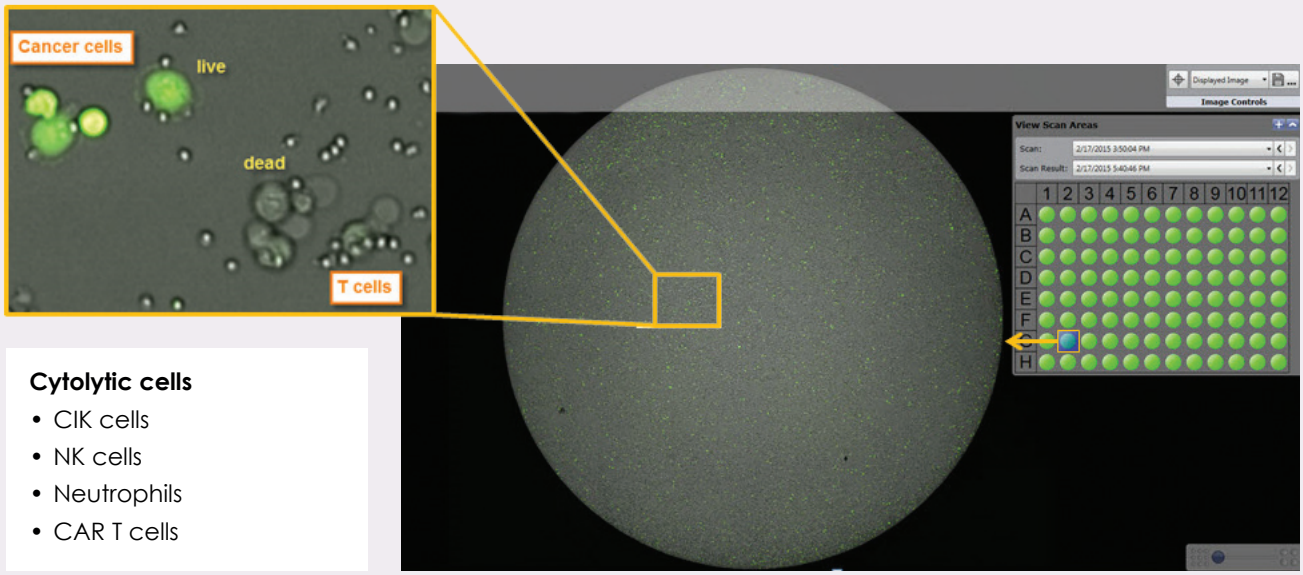

Cytolytic cells

- CIK cells
- NK cells
- Neutrophils
- CAR T cells

Fluorescent stains

- Fluorescent proteins - GFP, RFP
- Calcein AM
- Cell tracer dyes CFSE
- CellTrace™ dyes
- Viability dyes - PI, DAPI

5. Cell images are used by the Celigo software to count live tumor cells for each well.

Image tumor cells stained with Calcein AM

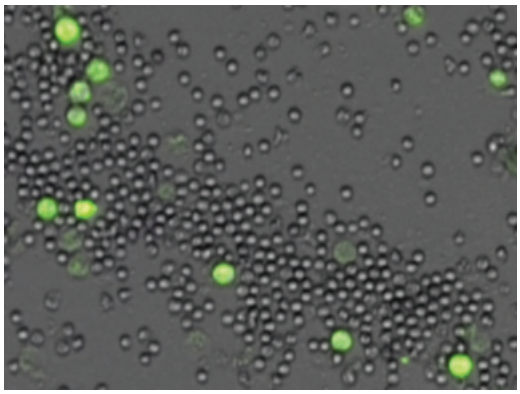

Count Calcein+ live tumor cells

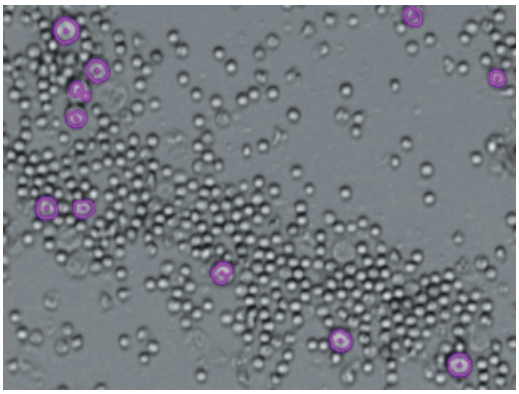

6. Direct cell counts for each well are reported in the plate map format

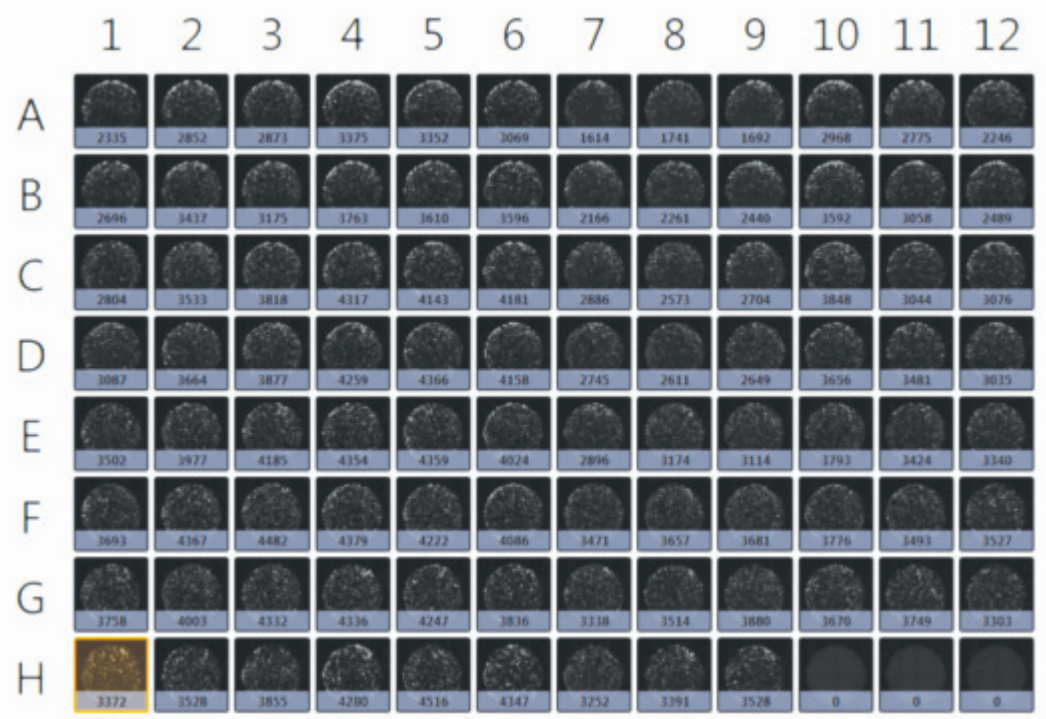

7. Each plate can be imaged multiple times during the killing process

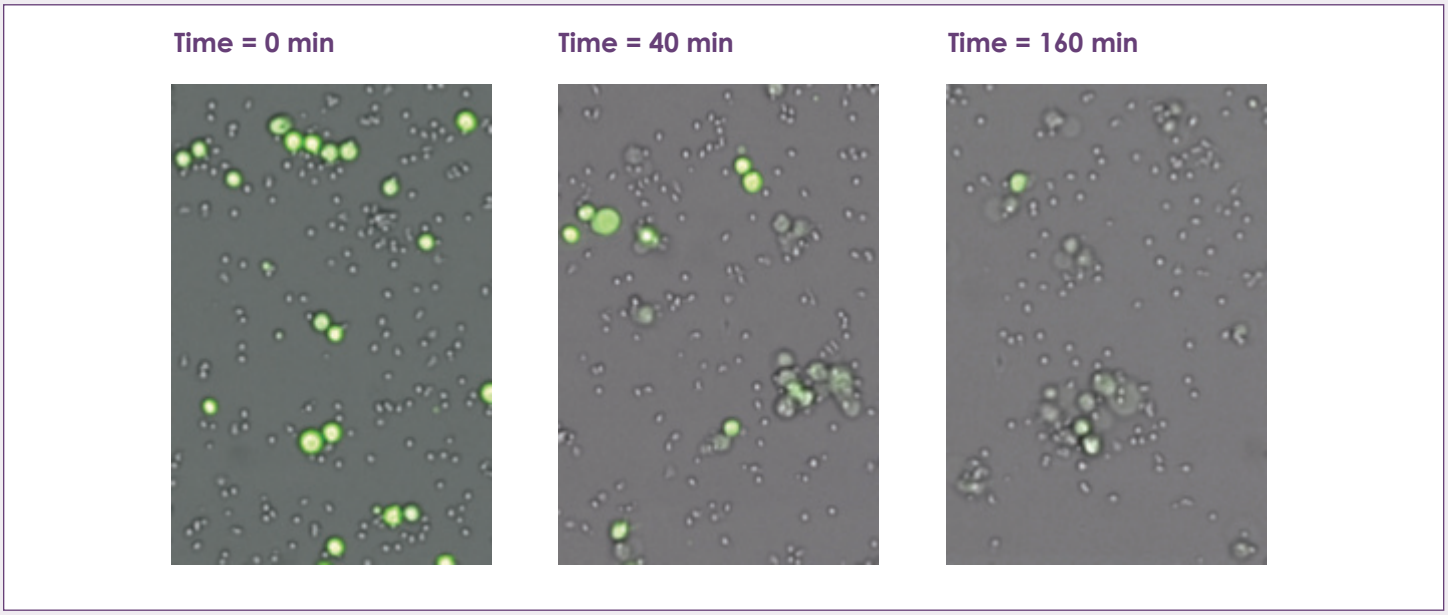

8. Numerical data output into .CSV file with plate level readout.

Live Count	1	2	3	4	5	6	7	8	9	10	11	12
A	27	214	883	1454	2094	2895	1234	2040	2702	3400	4158	4856
B	69	548	1405	2535	3197	3342	2097	3223	4608	6457	7123	6857
C	92	431	1297	2272	3303	3729	2173	3418	4764	6273	7158	8091
D												
E												
F	0	0	0	0	0	0	0	1	0	0	0	0
G												
H	3178	3442	4034	4056	3855	4119	9609	9458	9855	9836	9407	9418

9. Total cell count, live cell count, % live cell count and other parameters are generated for each well

General

Scan Area Location:	**C2**
% LIve:	**3.14%**
Live Count:	**1954**
Total Count:	**62203**
% Well Sampled:	**100.00%**
AVG Live Mean Intensity:	**105.22**
SD of Live Mean Intensity:	**28.36**
AVG Live Integrated Intensity:	**15,178.03**
SD of Live Integrated Intensity:	**11,016.99**
AVG Total Mean Intensity:	**113.75**
SD of Total Mean Intensity:	**22.25**
AVG Total Integrated Intensity:	**3,897.03**
SD of Total Integrated Intensity:	**3,812.26**

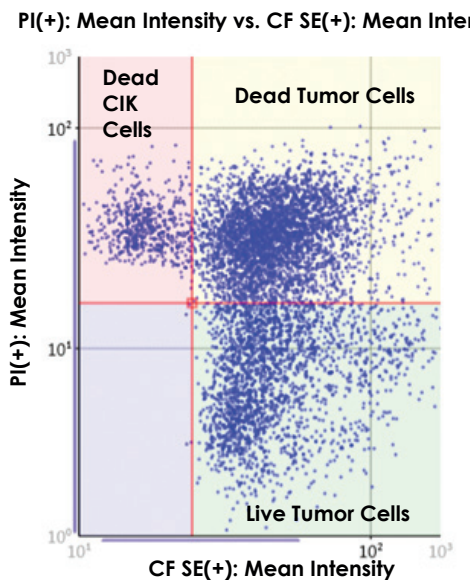

Quantification of Natural Killer Cell-Mediated Cytotoxicity Over 4 Hours with Multiple Time Point Measurement

Celigo Experimental Protocol

Target cells are collected and stained with Calcein AM (10 µM) → **Plate the Target cells at 10,000 cells/well** → **Collect Effector NK cells and add to 96-well plate at different E:T ratios** →

% Lysis Calculation for Cytotoxicity Measurement

- Count # of live Target cells (Calcein AM positive) in wells with Effector cells
- Count # of live Target cells (Calcein AM positive) in wells without Effector cells (control)

$$\%\ \text{Lysis} = \left[\frac{n_{CAM^+\_t0} - n_{CAM^+\_t}}{n_{CAM^+\_t0}}\right]_{treated} - \left[\frac{n_{CAM^+\_t0} - n_{CAM^+\_t}}{n_{CAM^+\_t0}}\right]_{control}$$

Experiment Design

E:T	1	2	3	4	5	6	7	8	9	10	11	12
A	10:1	5:1	2.5:1	1.3:1	0.6:1	0.3:1	10:1	5:1	2.5:1	1.3:1	0.6:1	0.3:1
B	10:1	5:1	2.5:1	1.3:1	0.6:1	0.3:1	10:1	5:1	2.5:1	1.3:1	0.6:1	0.3:1
C	10:1	5:1	2.5:1	1.3:1	0.6:1	0.3:1	10:1	5:1	2.5:1	1.3:1	0.6:1	0.3:1
D												
E	IMR32						K562					
F	Maximum Release Control						Maximum Release Control					
G												
H	Spontaneous Release Control						Spontaneous Release Control					

- IMR32 (Adherent) and K562 (Suspension) target cells are used to demonstrate the NK Cell-mediated cytotoxicity detection method using Calcein AM staining for direct cell counting
- The Effector-to-Target (E:T) ratio will be 10:1, 5:1, 2.5:1, 1.3:1, 0.6:1, and 0.3:1

- The Maximum Release uses Triton X100 to lyse all cells and release the Calcein AM fluorescent molecules
- Live Target cells are automatically counted at each E:T ratio from t = 1 - 4 hours
- Cell images at 4 hours for K562 cells

Control

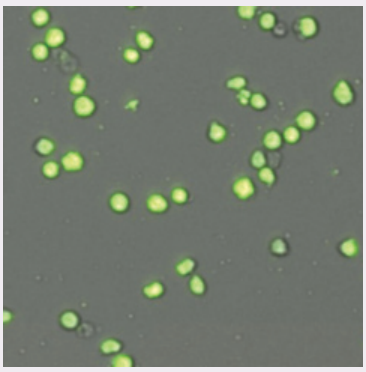

E:T = 0.6:1

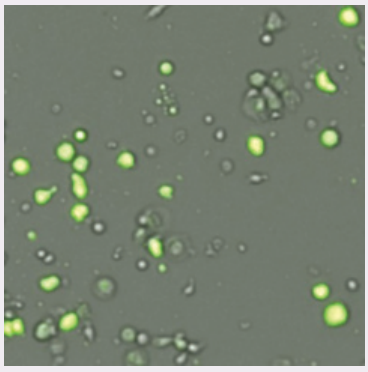

E:T = 5:1

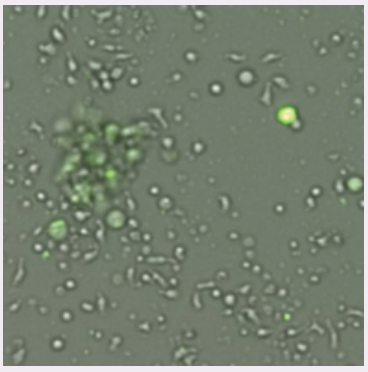

E:T Ratio and Time Dependant Cytotoxicity of K562

- The example Calcein+ fluorescent images are the K562 Target cells at t = 4 hours
- The resulting fluorescent images showed increase in Calcein AM positive Target cells as E:T ratio decreased

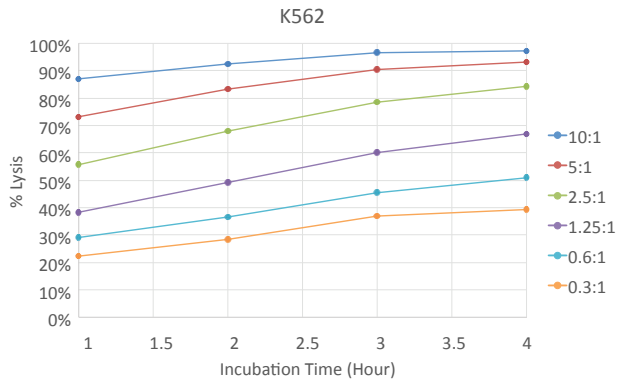

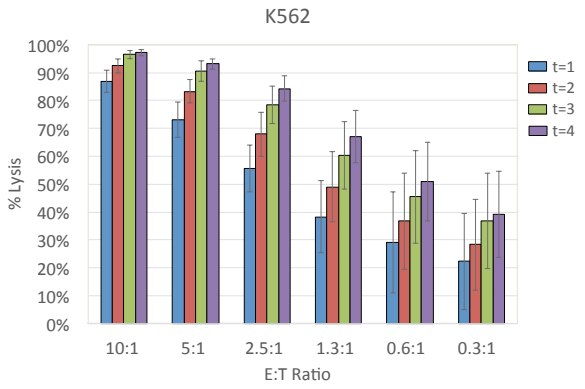

- The live K562 suspension cells were directly measured using the Celigo
- The number of Calcein AM positive cells was counted at each hour and used to calculate the % lysis for each E:T Ratio
- By analyzing the time course data of K562, we can see that the % lysis difference between the E:T Ratios is much smaller in comparison to IMR32

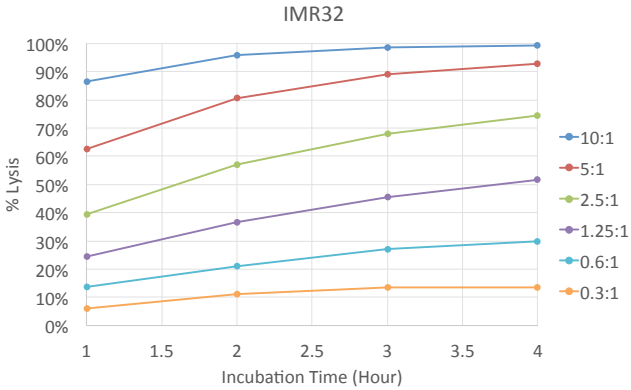

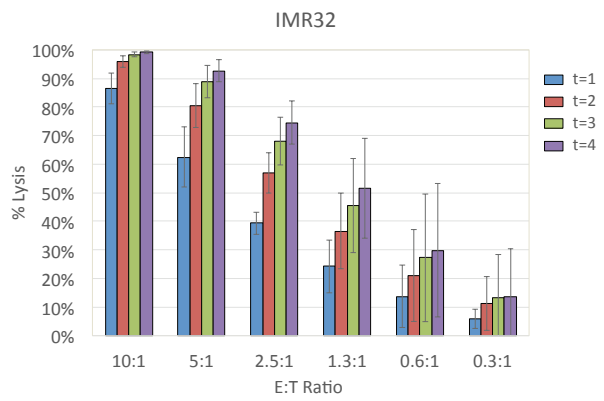

- The live IMR32 adherent cells were directly measured using the Celigo without trypsinization
- The number of Calcein AM positive cells was counted at each hour and used to calculate the % lysis for each E:T Ratio
- By analyzing the time course data of IMR32, we can see that there is a large % lysis difference between the E:T Ratio

Antibody-Dependent CIK-Mediated Cytotoxicity Using CFSE and PI

Fluorescent and Bright-Field Cell Images and Overlay for CFSE and PI

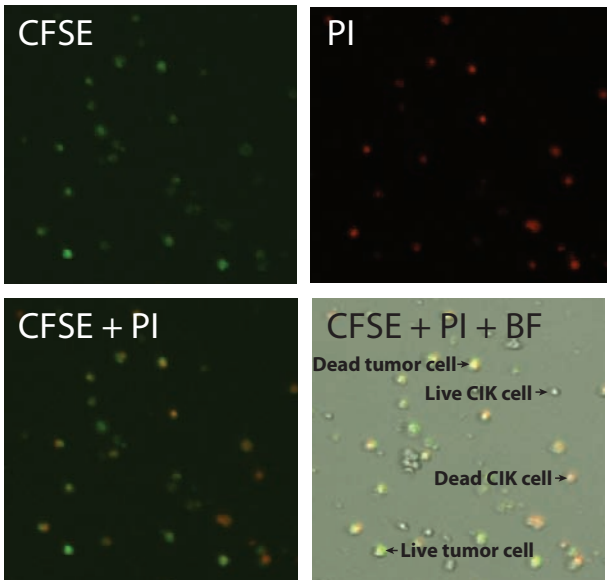

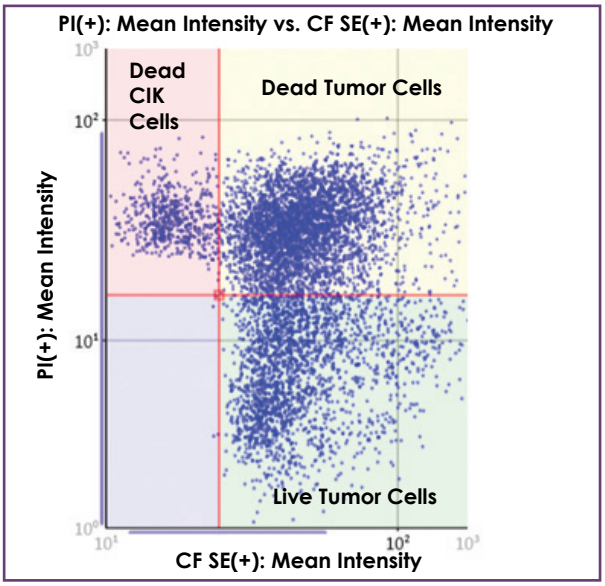

- Live tumor cells (CFSE+PI-)
- Dead tumor cells (CFSE+PI+)
- Live Effector cells (CFSE-PI-)
- Dead Effector cells (CFSE-PI+)

- The fluorescent intensities of CFSE and PI are plotted directly in the Celigo Software
- Quadrant LR indicates the live tumor cells
- Quadrant UR indicates the dead tumor cells
- Quadrant UL indicates the dead CIK effector cells

Antibody Concentration Dependent Cytotoxicity

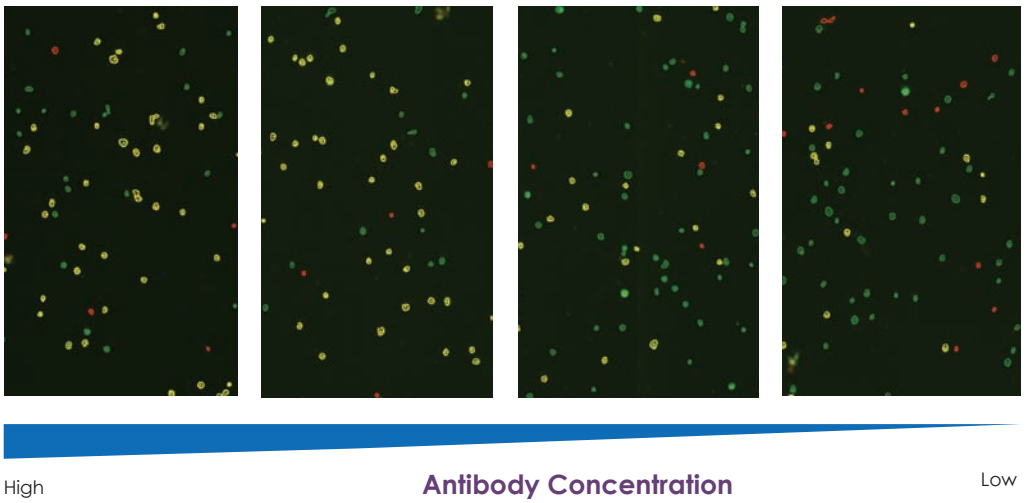

Cytotoxicity Assay Using Bright-field Morphological Confluence Assay

Direct Cell Killing Effect with Drug Concentration Curve

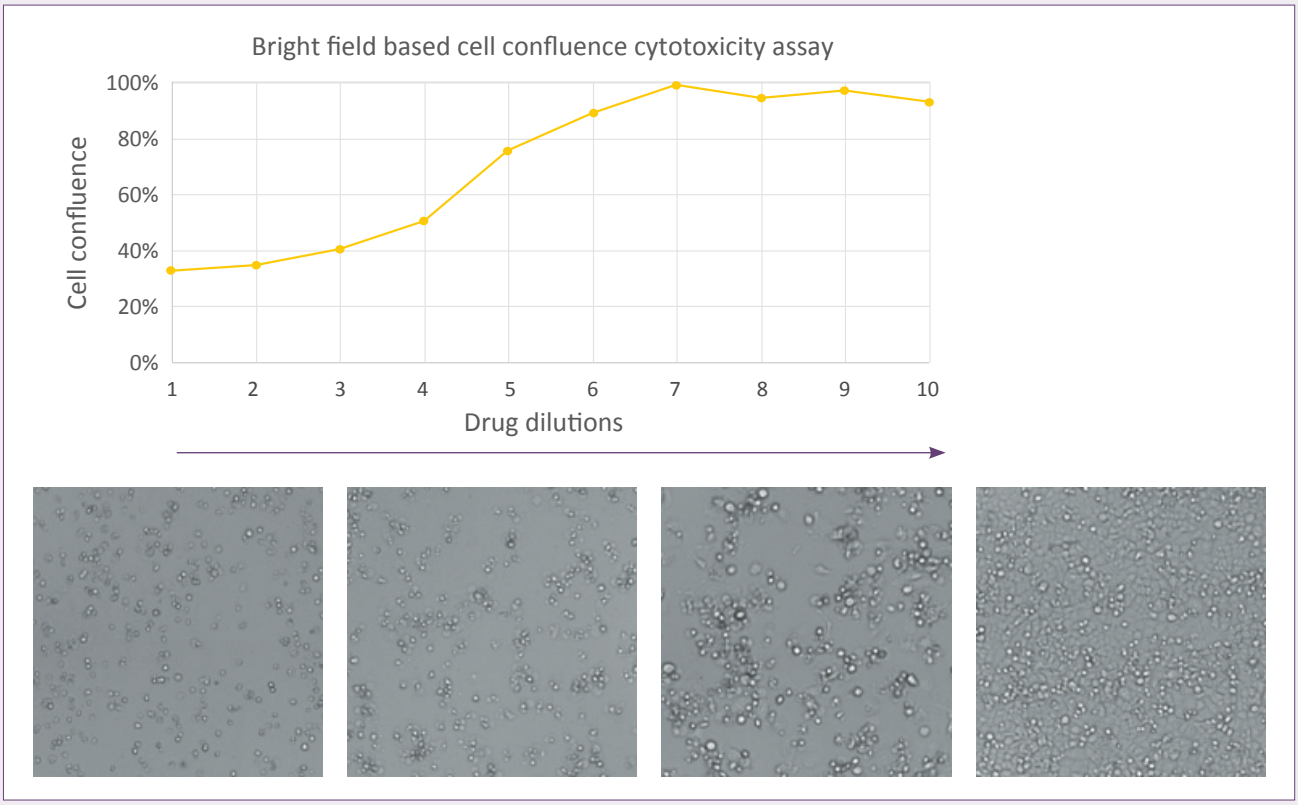

- The captured images show an increase of cell confluence with increased drug dilution.
- Celigo software produces cell growth curves for each drug treated sample. (not shown here)

Confluence Measurements for a Multi-drug Cytotoxicity Assay

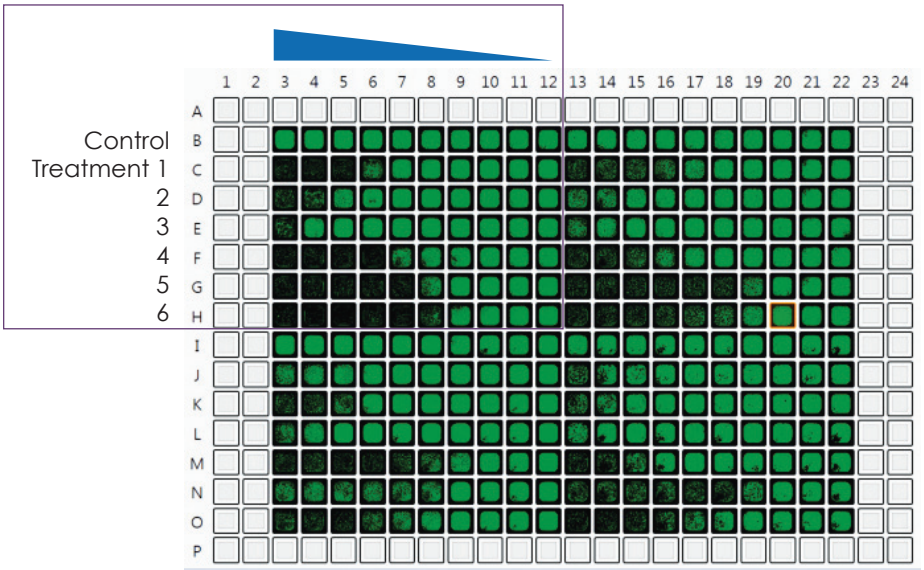

Drug treatment, concentration dependent cytotoxicity is represented by well level confluence measurement in a 384-well plate.

Green color indicates the level of confluence per well.

Traditional Methods vs. Natural Killer - Cell-Mediated Cytotoxicity Detection Methods

Traditional Cell-Mediated Cytotoxicity Detection Methods

Detection Method	Description	Existing Issues
Radioactivity Release	Measure release or radiolabels, 51Cr, 101In in the supernatant	Handling hazardous material and indirect measurement of cell death
Fluorescence Release	Measure release of Calcein AM fluorescent molecules in the supernatant	Indirect measurement of cell death, end-point assay only
LDH Release	Measure release of cytosolic enzyme in the supernatant	Indirect measurement of cell death, end-point assay only
Luciferase Reporter Assay	Measure luciferase as the cells die	Indirect measurement of cell death
Flow Cytometery	Measure number of viable cells and viability in the sample	Cannot perform in plates, must trypsinize for adherebt cells

Celigo Benefits for Direct Cell Counting ADCC

- Time-course tracking of % lysis can eliminate the need of multiple controls, and the effect of non-uniform cell seeding in the final cytotoxicity calculation.
- Adherent cells can be measured and analyzed directly in the plate without trypsinization.
- The number of cells used is significantly reduced compared to other release assays and Flow Cytometry, from 100,000 to 10,000 target cells.
- The visual observation of Cell-Mediated, ADCC, or CDC effect on tumor cells provides additional information on the functionality of antibodies or complements.

Celigo Assays for Immuno-Oncology

- **Direct cell counting and confluence measurement using bright-field**
  - Antibody-mediated cell killing (cell proliferation)
- **Direct cell counting method using Calcein AM (or GFP, RFP)**
  - NK cell-mediated cytotoxicity
  - NK ADCC
  - Neutrophil ADCC
  - CDC
- **Direct cell counting method using tracer dye, fluorescent protein, viability dye**
  - CIK ADCC
  - CAR T cell-mediated cytotoxicity

Cellometer® Simply Counted | Celigo® S Image Cytometer

Celigo® in Publications

Celigo Brightfield Assays

1 Singh A, Lun X, Jayanthan A, et al. (2013) Profiliing Pathway Specific Novel Therapeutics in Preclinical Assessment for CNS Atypical Teratoid Rhabdoid Tumors. *Molecular Oncology* 7(3): 497-512.

Cell growth inhibition/ cell toxicity. Three established cell lines (BT12, BT16 and KCCF1) from CNS atypical teratoid/rhabdoid tumors were treated with 129 different compounds. Cell survival and IC50 were determined using direct bright field counting.

2 Lesovaya E, Yemelyanov A, Kirsanov K, et al. (2013) Combination of a Selective Activator of the Glucocorticoid Receptor Compound A with a Protease Inhibitor as a Novel Strategy for Chemotherapy of Hematologic Malignancies. *Cell Cycle* 12(1): 133-44.

Cell toxicity for suspension cells. Treated cultured cells, lentivirus- transformed cells, and primary patient cells with drugs for 48 hours and observed cell growth.

3 Hoeksema KA, Jayanthan A, Cooper T, et al. (2011) Systematic in-Vitro Evaluation of the NCI/NIH Developmental Therapeutics Program Approved Oncology Drug Set for the Identification of a Candidate Drug Repertoire for MLL-Rearranged Leukemia. *OncoTargets and Therapy* 4: 149-68

A large drug screen study performed on 5 tumor cell lines. Cells growth was determined 96 hours post the addition of the drugs. The activity of each drug was compared to commonly used drugs in therapeutics for pediatric leukemia. The ratios of the drugs were plotted as a heat maps.

For selected drugs a dose response assay was performed. A serial dilution of drugs was added to the cells and cell survival measured.

Growth curves. Cells were incubated with a drug at a specific concentration and data collected every 24 hours for 4 days. Survival percentage was calculated by comparing the number of viable cells in treated wells to DMSO control.

4 Lesovaya EA, Yemelyanov AY, Kirsanov KI, et al. (2011) Antitumor Effect of Non-stroid Glucocorticoid Receptor Ligand CpdA on Leukemia Cell Lines CEM and K562. *Biochemistry* (Moscow) 76(11): 1242-52.

Cell toxicity for leukemia suspension cells (CEM and K562 cells). Cells were imaged 48 hours post drug treatment.

5 Feng L, Sun X, Csizmadia, et al. (2011) Vascular CD39/ENTPD1 Directly Promotes Tumor Cell Growth by Scavenging Extracellular Adenosine Triphosphate. *Neoplasia* 13(3): 206-16

Cell Confluence. siRNA transfected U251 cells were treated with multiple drugs and confluence was measured regularly for the next 400 hours.

6 Schulz R, Streller F, Scheel AH, et al. (2014) HER2/ErbB2 Activates HSF1 and Thereby Controls HSP90 Clients Including MIF in HER2-Overexpressing Breast Cancer. *Cell Death and Disease* 5: e980

Cell survival/ Cell Confluence. Cells were seeded (day 0) and cultured for 24 hrs, then treated with a drug for 24 hrs. Cell confluence measured for daily for the next 5 days and compared to untreated control cells.

7 Bian S, Sun X, Bai A, et al. (2013) P2X7 integrates PI3K/AKT and AMPK-PRAS40-mTOR signaling pathways to mediate tumor cell death. PLoS One 8(4)

Cell Growth Assay. MCA38 cells were treated with ATP for 1 hr and cell growth was assessed 24 hrs post treatment.

8 Fu X, Creighton CJ, Biswal NC, et al. (2014) Overcoming endocrine resistance due to reduced PTEN levels in estrogen receptor-positive breast cancer by co-targeting mammalian target of rapamycin, protein kinase B, or mitogen-activated protein kinase kinase. *Breast Cancer Research* 16(5): 430

Cell Growth Assay. Human breast cancer cell lines MCF7L, BT483, T47D were treated with multiple drugs and cell growth was monitored daily.

9 Jayanthan A, Ruan Y, Truong TH, Narendran A. (2014) Aurora kinases as druggable targets in pediatric leukemia: heterogeneity in target modulation activities and cytotoxicity by diverse novel therapeutic agents. *PLoS One* 9(7)

Cytotoxicity Assay. Multiple B and T-cell lines from acute lymphoblastic leukemia (ALL) , and acute myeloid leukemia (AML) lineages were examined for cytotoxicity in a 96-well plate format. Post treatment, cell survival and IC50 were determined using direct bright field cell counting.

10 Morrison G, Fu X, Shea M, et al. (2014) Therapeutic potential of the dual EGFR/HER2 inhibitor AZD8931 in circumventing endocrine resistance. *Breast Cancer Research and Treatment* 144(2): 263-672

Cell Growth Assay. Breast cancer cell lines MCF7 and T47D were treated with multiple pharmacological agents and an initial cell number was acquired on day 0. On day 6 post treatments, the change in cell growth was determined by comparing cell number on day 6 to cell number from day 0.

11 Landmann H, Proia DA, He S, et al. (2014)UDP glucuronosyltransferase 1A expression levels determine the response of colorectal cancer cells to the heat shock protein 90 inhibitor ganetespib. *Cell Death&Disease* 9(11)

Proliferation Assay. Eleven human colorectal cancer cell lines were seeded in a 12 well plate and treated with inhibitors. Cell confluence was measured every 24 hours for 4 days post initial treatment.

Stem Cells / iPS Cells Celigo Assays

1 Hua H, Shanq L, Martinez H, et al. (2013) iPSC-Derived B-Cells Model Diabetes Due to Glucokinase Deficiency. *Journal of Clinical Investigation*123(7): 3146-53

Cell Growth and immunostaining of iPSC and iPSC derived ß cells.

2 Sproul AA, Jacob S, Pre D, et al. (2014)Characterization and Molecular Profiling of PSEN1 Familial Alzheimers Disease iPSC Derived Neural Progenitors. *PLOS one9(1): e84547*

Hoescht and immunofluorescence staining of iPSC cells derived from human fibroblasts. Multiple stains were performed including the detection of nestin, a neural progenitor marker.

3 Tingen CM, Kiesewetter SE, Jozefik J. (2011) A Macrophage and Theca Cell-Enriched Stromal Cell Population Influences Growth and Survival of Immature Murine Follicles in Vitro. *Society for Reproduction and Fertility* 141(6): 809-20.

Cell Surface marker detection of CD11b and counterstained with Hoescht. Adherent ovarian stromal cells at day 4, 8, or 12 were stained with FITC anti- CD11b and Hoescht.

4 Golipour A, David L, Liu Y, et al. (2012)A late transition in somatic cell reprogramming requires regulators distinct from the pluripotency network. *Cell Stem Cell* 11(6): 769-782

iPSC reprogramming. Secondary MEFs were transfected, drug treated and allowed to grow. Cells were counterstained with DAPI, and colonies were examined for the presence of Dppa4.

Fluorescent Celigo Assays

1 Al-Kasspooles MF, Williamson SK, Henry D, et al. (2013) Preclincal Antitumor Activity of a Nanoparticulate SN38. *Journal of Investigative New Drugs* 31(4): 871-80

Cell Viability using PI and Cell Proliferation. Initial viability was assessed after an overnight incubation, and then a drug was added in a dose dependent manner. Cell viability and cell growth was tested 24, 48, and 72 h after the addition of the drugs.

2 Li D, Gaedigk R, Hart SN, et al. (2012) The Role of CYP3A4 mRNA Transcript with Shortened 3'-Untranslated Region in Hepatocyte Differentiation, Liver Development and Repsonse to Drug Induction. *Molecular Pharmacology* 81(1): 86-96

Transfection efficiency of HepaRG cells by detecting RFP positive cells.

3 Smith KT, Sardiu ME, Martin-Brown SA, et al. (2012) Human Family with Sequence Similarity 60 Member A (FAM60A) Protein: a New Subunit of the Sin3 Deacetylase Complex. *Molecular Cell Proteomic* 11(12): 1815-28

BrdU Cell Proliferation of A549 and HepG2 cells. Cells were also costained with DAPI.

4 Yoshida S, Nabzdyk CS, Pradhan L, et al. (2011) Thrombospondin-2 Gene Silencing in Human Aortic Smooth Muscle Cells Improves Cell Attachment. *Journal of the American College of Surgery* 213(5):668-76

Wound Healing/Migration Assay. HAoSMC cells were plated and allowed to grow. A scratch was applied across the plate creating a "wound". Initial position of the cells was determined with Hoechst staining. Cell migration was monitored over the next several days.

5 Sirmaci A, Erbek S, Price J, et. Al. (2010) A Truncating Mutation in SERPINB6 is Associated with Autosomal Recessive Nonsyndromic Sensorineural Hearing Loss. *The American Journal of Human Genetics* 86(5): 797-804

GFP to measure the number and intensity of expressed recombinant protein in HeLa cells. LysoTracker (Red) intensity, to evaluate lysosomal integrity.

6 Li J, Ding SC, Cho H, et al. (2013) A Short Hairpin RNA Screen of Interferon-Stimulated Genes Identifies a Novel Negative Regulator of the Cellular Antiviral Response. *Mbio*. 4(3): e00385-13

Viral Infectivity. Transfected HeLa cells were infected with West Nile Virus (WNV). Cells were fixed and stained for WNV envelope protein as well as DAPI. Infectivity was measured as the percentage of infected cells from the total cell counts.

7 He X, Berland R, Mekasha S, et al. (2013) The sst1 Resistance Locus Regulates Evasion of Type 1 Interferon Signalling by Chlamydia pneumoniae as a Disease Tolerance Mechanism. *PLOS one: Pathogens* 9(8): e1003569

Cytotoxicity and Cell Viability using Hoechst and PI. BMDM cells were plated and pre-treated with neutralizing antibodies and infected with C.pneumoniae. Cytotoxicity was determined over 24, 48, and 72 hours as a ratio of dead cells to the total cell number using PI and Hoechst staining.

8 Giovannini M, Bonne NX, Vitte J, et al. (2014) mTORC1 Inhibition Delays Growth of Neurofibromatosis Type 2 Schwannoma. *Neuro-Oncology* 16(4): 493-504

Cell Surface Area. Primary human schwannoma cells were treated with multiple drugs over a period of 20 days. Cells were then fixed with 4% PFA and stained with anti-S100 protein as well as Hoechst. An average of 450 cells per 12 well plate and an average of 900 cells per 24 well plate were quantified.

9 Ferree AW, Trudeau K, Zik E, et al. (2013) MitoTimer Probe Reveals the Impact of Autophagy, Fusion and Motility on Subcellular Distribution of Young and Old Mitochondrial Protein and on Relative Mitochondrial Protein Age. *Autophagy* 9(11): 1887-96

Autophagy using MitoTimer. Looked at average Red/Green fluorescence intensities in drug treated MEF and COS cells.

10 Morrison G, Fu X, Shea M, et al. (2014) Therapeutic potential of the dual EGFR/HER2 inhibitor AZD8931 in circumventing endocrine resistance. *Breast Cancer Research and Treatment* 144(2): 263-672

Proliferation Assay. Proliferation of treated MCF7 and T47D cells was measured using Click-iT EdU assay.

Apoptosis Assay. Treated MCF7 cells were stained with annexin V –FITC and percent of apoptotic cells for each condition was assessed.

11 Wang YC, Morrison G, Gillihan R, et al. (2011) Different mechanisms for resistance to trastuzumab versus lapatinib in HER2-positive breast cancers--role of estrogen receptor and HER2 reactivation. *Breast Cancer Research and Treatment* 13(6): R21

Proliferation Assay. Proliferation of treated and resistant BT474 cells was measured using Click-iT EdU assay.

Apoptosis Assay. Treated and resistant BT474 cells were stained with annexin V –FITC and percent of apoptotic cells for each condition was assessed.

12 Chen HY, Yang YM, Stevens BM, Noble M. (2013) Inhibition of redox/Fyn/c-Cbl pathway function by Cdc42 controls tumour initiation capacity and tamoxifen sensitivity in basal-like breast cancer cells. *EMBOmolecular medicine* 5(5): 723-736

Cell Viability. Treated and untreated basal-like breast cancer cells were stained with Calcein-AM and propiduim iodide to determine cell viability.

Reactive Oxygen Species (ROS) Detection. Treated and untreated basal-like breast cancer cells were stained with CM-H2DCFDA and the fluorescence intensity for ROS(+), and ROS(-) samples determined

13 Nabzdyk CS, Chun M, Pradhan Nabzdyk L, et al. (2012) Differential susceptibility of human primary aortic and coronary artery vascular cells to RNA interference. *Biochemical and Biophysical Research Communications* 425(2): 261-265

Transfection Efficiency. Human aortic and coronary endothelial and smooth muscle cells were seeded in a 96 well plate and transfected. Hoechst staining was performed for nuclei detection and red (PE) filter was used to detect siGLO Red signal from positively transfected cells.

14 Ronda C, Pedersen LE, Hansen HG, et al. (2014) Accelerating genome editing in CHO cells using CRISPR Cas9 and CRISPy, a web-based target finding tool. *Biotechnology and Bioengineering* 111(8): 1604-1616

Transfection Effeciency. CHO-K1 cells were transfected with a pmaxGFP plasmid. To determine transfection efficiency, a bright field image of the total cell population was acquired along with the GFP positive cells.

15 Xu C, Tabebordar M, Iovino S, et al. (2013) A zebrafish embryo culture system defines factors that promote vertebrate myogenesis across species. *Cell* 155(4): 909-921

High Throughput Screening. Double-transgenic, with a GFP and m-Cherry reporter, disassociated blastomere cells from zebra fish were seeded in a 384-well plate. After an incubation period, cells were imaged and analyzed for the expression of GFP and m-Cherry fluorescent signals.

16 Tingen CM, Kiesewetter SE, Jozefik J, et al. (2011) A macrophage and theca cell-enriched stromal cell population influences growth and survival of immature murine follicles in vitro. *Reproduction* 141(6): 809-820

Immunocytochemistry. Mouse ovarian stroma cells were stained with Hoechst and FITC anti-CD11b antibody.

17 Lund AM, Kildegaard HF, Petersen MB, et al. (2014) A versatile system for USER cloning-based assembly of expression vectors for mammalian cell engineering. *PLoS One* 9(5)

Transfection Efficiency. Transfected CHO-S cells were stained with Hoechst33342 and percent of GFP positive cells was determined.

18 Golipour A, David L, Liu Y, et al. (2012)A late transition in somatic cell reprogramming requires regulators distinct from the pluripotency network. *Cell Stem Cell* 11(6): 769-782

Immunocytochemistry. Secondary mouse embryonic fibroblasts (MEFs) were stained and scored for positive alkaline phosphatase areas. The cells were also counterstained with DAPI.

19 Yang CC, Chung A, Ku Cy, et al. (2014) Systems analysis of the prostate tumor suppressor NKX3.1 supports roles in DNA repair and luminal cell differentiation. *F1000Research* 3(115)

Proliferation. Transduced LH cells were seeded in a 384-well plate and proliferation examined by looking at the rate of Click iT EdU Alexa Fluor 594 incorporation versus total number of cells which were counterstained with DAPI.

20 Trapnell C, Cacchiarelli D, Grimsby J, at al. (2014) The dynamics and regulators of cell fate decisions are revealed by pseudotemporal ordering of single cells. *Nature Biotechnology* 32(4): 381-386

Immunocytochemistry. Human skeletal muscle myoblasts were stained with fluorescent antibodies against muscle MYH2, MEF2C, and phospho-histone H3 and counterstained with DAPI.

21 Escribano-Díaz C, Orthwein A, Fradet-Turcotte A, et al. (2013) A cell cycle-dependent regulatory circuit composed of 53BP1-RIF1 and BRCA1-CtIP controls DNA repair pathway choice. *Molecular Cell* 49(5): 872-883

Immunocytochemistry. Transfected U2OS cells were fixed and stained for RPA32 immunofluorescence. Percent of RPA32 positive cells was calculated based on the total number of DAPI-positive counterstained cells.

22 Hua H, Shang L, Martinez H, et al. (2013) iPSC-derived ß cells model diabetes due to glucokinase deficiency. *The Journal of Clinical Investigation* 123(7): 3146-3153

Immunocytochemistry. Reprogrammed to iPS cells were stained with multiple fluorescent stem cell markers and examined for positive signals.

23 Proschel C, Stripay JL, Shih CH, et al. (2014) Delayed transplantation of precursor cell-derived astrocytes provides multiple benefits in a rat model of Parkinsons. *EMBO Molecular Medicine* 6(4): 504-518

Immunocytochemistry. Immunostaining and detection of cortical and dopaminergic mid-brain neurons

24 Sproul AA, Jacob S, Pre D, et al. (2014) Characterization and molecular profiling of PSEN1 familial Alzheimer's disease iPSC-derived neural progenitors. *PLoS One* 9(1)

Immunocytochemistry. Reprogrammed to iPS cells were stained with multiple fluorescent stem cell markers and examined for positive signals

25 Shih CH, Lacagnina M, Leuer-Bisciotti K, Proschel C. (2014) Astroglial-derived periostin promotes axonal regeneration after spinal cord injury. *Journal of Neuroscience* 34(7): 2438-2443

Confluence of immunostained primary dorsal root ganglion neurons

26 Holembowski L, Kramer D, Riedel D, et al. (2014) TAp73 is essential for germ cell adhesion and maturation in testis. *Journal of Cell Biology* 204(7): 1173-1190

Transduction efficiency of primary rat Sertoli cells by measuring the percent of GFP positive cells.

27 Chen HY, Yang YM, Han R, et al. (2013) MEK1/2 Inhibition Suppresses Tomixfen Toxicity on CNS Glial Progenitor Cells. *The Journal of Neuroscience* 33(38): 15069-74

Cell number and Viability using Calcein AM/PI of drug treated and control human astrocyte progenitor cells/oligodendrocyte precursor cells.

Celigo 3D Tumor Spheroids, Cancer Stem Cell Colony Formations

1 Fu X, Creighton CJ, Biswal NC, et al. (2014) Overcoming endocrine resistance due to reduced PTEN levels in estrogen receptor-positive breast cancer by co-targeting mammalian target of rapamycin, protein kinase B, or mitogen-activated protein kinase kinase. *Breast Cancer Research* 16(5): 430

Tumorsphere quantification. Tumorsphere size and number from a breast cancer cell line were measured using bright field imaging as well as red fluorescence imaging.

2 Neradugomma NK, Subramaniam D, Tawfik OW, et al. (2014) Prolactin signaling enhances colon cancer stemness by modulating Notch signaling in a Jak2-STAT3/ERK manner. *Cancinogenesis* 35(4): 795-806

Spheroid quantification. Colon cancer cell lines HT29, HCT116, SW480, SW620, and FHC were treated with inhibitors and seeded in a 6-well plate. After several days, the cells were imaged for spheroid formation. Spheroid number and size was determined using bright field imaging.

3 Ponnurangam S, Mammen JM, Ramalingam S, et al. (2012) Honokiol in combination with radiation targets notch signaling to inhibit colon cancer stem cells. *Molecular Cancer Therapeutics* 11(4): 963-972.

Colonosphere quantification. HCT116 and SW480 cells were treated, seeded, and analyzed 7 days later for the number and size of formed colonospheres.

4 Borrego-Diaz E, Terai K, Lialyte K, et al. (2012) Overactivation of Ras signaling pathway in CD133+ MPNST cells. *Journal of Neuro-oncology* 108(3):423-434

Spheroid quantification. CD133+ enriched population from S805 MPNST cells were seeded in a 6-well plate. The formation malignant peripheral nerve sheath tumor (MPNST) of spheroids was assessed throughout the incubation period.

5 Guo WM, Loh XJ, Tan EY, et al. (2014) Development of a magnetic 3D spheroid platform with potential application for high-throughput drug screening. *Molecular Pharmaceutics* 11(7): 2182-2189

Spheroid quantification. Measured the growth kinetics of drug treated MCF-7speroids utilizing bright field imaging.

Cellometer® Simply Counted

Celigo® S Image Cytometer

Innovation and Expertise in the Science of Cell Counting

On-Site Demonstrations are a convenient way to evaluate the Celigo S System. We have regional demonstration laboratories where you can have an hands on session to test your cells. Another option is to have an experienced Applications Specialist visit your lab with the Celigo S System for a hands-on session to test your application.

Technical Seminars are an excellent way to introduce Celigo S Systems to a lab group or collaborators in different laboratories within an organization. A trained biologist will discuss and demonstrate the capabilities and advantages of the Celigo S Image Cytometer for cell viability and cell-based assays.

Schedule a FREE on-line demonstration, on-site demonstration or technical seminar with a Nexcelom Applications Specialist today.

Call 978-327-5340 or E-mail info@nexcelom.com

Nexcelom Bioscience

For more information, visit www.nexcelom.com

Contact us at:
Nexcelom Bioscience
360 Merrimack Street, Building 9
Lawrence, MA 01843, USA

Email: info@nexcelom.com
Phone: 978.327.5340
Fax: 978.327.5341

Cell Counters, Cell Analysis Systems & Image Cytometry
Nexcelom offers a wide range of imaging systems developed and optimized for specific applications and cell types.

www.nexcelom.com/products

Cellometer® Simply Counted

Celigo® S Image Cytometer

1001273 RevC 06/15